

## **Response to the Reviewers**

The authors are very grateful to the reviewers for their constructive comments. Based on their input, the paper has been significantly revised and improved. The revised version is part of this reply letter.

We avoided to highlight the many, many changes (in color or bold) triggered and recommended by the reviewers to facilitate reading of the revised manuscript.

Let us start with a general remark:

The reviewers suggest to merge the papers: Ansmann et al., 2018 (paper 1) and Haarig et al. (paper 2).

We think this is not a good solution for the following reasons!

Paper #1 (revised version) deals with observation of the record-breaking fire event using spatial technologies and spatial mapping, we investigate the origin of the smoke observed over central Europe and illuminate the transport across the Atlantic, and present time series and maps of AOT observation using different instruments (MODIS, OMI, AERONET, EARLINET lidars). Such events can be hardly monitored by conventional means. Highlight are the height-resolved lidar measurements because only profiling techniques allow us to clearly see and quantify the stratospheric perturbation and the record-breaking contamination. In contrast to paper #1, paper #2 deals mainly with lidar-derived spectral optical, microphysical, and morphological/aerosol shape/type properties of the smoke. So we have two quite different papers.

Paper #1 highlights and documents this historical, record-breaking stratospheric smoke event, whereas paper #2 highlights and focuses on unique lidar aspects, i.e., on smoke profiling with a world-wide unique triple-wavelength polarization/Raman lidar providing lidar ratio and depol ratio profiles at 355, 532, and 1064 nm, and lidar inversion results (size distribution, single scattering albedo, shape characteristics). Such a set of optical profile data has never been presented before.

We would overload the article if we put together the contents of the two papers, even after reduction and condensation of the information content. There are simply too many features and facts worthwhile to be published.

But! We realize that we did a mistake: We selected (almost) the same title for the two quite different papers. The titles are now changed and thus corroborate the difference, and that both papers are stand-alone papers.

Paper #1: Extreme levels of Canadian wildfire smoke in the stratosphere over central Europe on 21-22 August 2017

Paper #2: Depolarization and lidar ratios at 355, 532, and 1064 nm and microphysical properties of aged tropospheric and stratospheric Canadian wildfire smoke

Forced by the comments of the reviewers, we rearranged the papers and fully separated the contents of the two papers, they are practically no longer overlapping regarding the presented results.

## **Now to paper #1.**

Our answers are given in bold. The paper is significantly modified and many parts were re-written based on the reviewers comments

A short summary of the main changes in the beginning:

- We added further satellite observations (MODIS 550 nm AOT and OMI 354 nm Aerosol Index from western Canada to Europe) to show the smoke situation (for August 2017) over North America, the North Atlantic, and Europe.
- Therefore, we extended Fig. 1: Besides Fig. 1a (old Fig.1), now we added Fig1b (OMI 354 nm AI map), and Fig.1c (MODIS 550 nm AOT map). We added these figure to highlight the spatial pattern and transport of aerosols to Europe as seen from space. And this event is so unique that we see it.
- We added new Polly observations, performed at Hohenpeissenberg (near Munich). Now we show lidar observations (extinction profiles up to 17 km height) at Hohenpeissenberg, Leipzig, and Kosetice (southeast of Prague) in a new Fig.4 (profiles) and new Fig. 5 (map to indicate the stations, and stratospheric 532 nm AOT over the stations). We extended the studied period (now 21-22 August, not only 22 August).
- We introduced a new section (Sect. 4: Discussion). In Sect. 4, we discuss and compare the properties and features of strong (Pinatubo) and moderate volcanic eruptions and extreme and typical pyroCB smoke events on the stratospheric conditions observable at northern midlatitudes. For this we introduced a new Table 1 showing and summarizing the main features of the different events. Because of Table 1 (and the references mentioned in the table), new literature is added to the references.
- We removed Fig. 2 (photos) and Fig. 8 (a similar figure is discussed in paper #2).
- We moved Fig. 9 (depol ratio spectra comparison, fine-mode smoke vs fine-mod dust) to paper #2.
- We extended the AERONET part (Sect. 3.5). In addition to the presentation and discussion of the Leipzig AERONET observations, we now discuss the obvious bias in the AERONET AOT observations, caused by multiple scattering in case of a sun photometer with a receiver view angle of  $1.2^\circ$ , i.e., 20 mrad. At these unusual conditions with a dense aerosol layer 12-17 km away from the photometer, the effectively measured 500 nm AOT was 30%-50% lower than the 532 nm AOT derived from the lidar measurements. This systematic bias was found for all lidar stations (Leipzig, Hohenpeissenberg, Kosetice/Brno). We summarized the findings in a new Table 2.

Now the step-by-step reply:

## **Reviewer #1:**

General comments:

This article is an introductory paper (part 1) dealing with the analysis of an extreme event of smoke particles advected from Canada to Central Europe. The work presented here is valuable, especially because high quality and trustworthy climate modeling is only possible in close connection with observations as the ones presented here. In general, the article is writing but my main concern is the reason why this work has been split in two different papers. I recommend merging them into one more robust and complete paper.

***See our argumentation above. We prefer to keep the two-paper structure, however with practically no overlap (anymore) of the presented findings and results. The papers deal with very different aspects. Based on this comment, the paper was re-written and additional analyses introduced.***

Specific comments:

The first part of section “Introduction” seems more like results and you should move to the section “Observations”. Because this study is part of the EARLINET network, it would be nice to include a paragraph summarizing the EARLINET findings on this type of particle layers, especially coming from Canada. As suggestion, some these papers are listed below:

Lucja Janicka, Iwona S. Stachlewska, Igor Veselovskii, Holger Baars, Temporal variations in optical and microphysical properties of mineral dust and biomass burning aerosol derived from daytime Raman lidar observations over Warsaw, Poland, *Atmospheric Environment*, 169, 162-174, 2017.

Ortiz-Amezcu, P., Guerrero-Rascado, J. L., Granados-Muñoz, M. J., Benavent-Oltra, J. A., Böckmann, C., Samaras, S., Stachlewska, I. S., Janicka, L., Baars, H., Bohlmann, S., and Alados-Arboledas, L.: Microphysical characterization of long-range transported biomass burning particles from North America at three EARLINET stations, *Atmos. Chem. Phys.*, 17, 5931-5946, <https://doi.org/10.5194/acp-17-5931-2017>, 2017.

***We shortened the lengthy introduction (as suggest by reviewer #2). But we would like to mentioned a few results (20 times stronger than Pinatubo) in the beginning of the Introduction to attract readers who know about the major Pinatubo volcanic event. Many papers start in this way.***

***We want to focus on stratospheric smoke only, because only this aspect is very new and provides the record-breaking touch. So, we leave out to discuss the EARLINET findings and observations (they all deal with tropospheric smoke). We would like to emphasize that paper #2 contains an extended literature review with many EARLINET smoke contributions (to lidar ratio and depolarization ratio aerosol characterizations). So, the summary of EARLINET findings is given in paper #2.***

***The two papers (Janicka et al, Ortiz et al.) are nice, relevant, and will be considered now in paper #2. Ortiz et al is already considered in paper #2. But we will add the interesting paper of Janicka et al.***

Page 2, line 28. AOT is a quantify depending on the wavelength. It is necessary to specify the wavelength referred to.

**We agree, and try to mention that we have 500 nm (AERONET), 550 nm (MODIS) and 532 nm (lidar).**

Section “Instrumentation” contains more than solely instrumental information. In contrast, methodology details are given here. Please, consider rename this section. Instrument section should reorganized due to in this paper (part 1) detailed lidar analysis is not the focus. Thus, I recommend to present first Sun-photometer, then MODIS and finally lidar system.

***We changed the title and subtitles of Section 2 accordingly. But we did not change the order of presentation. The paper belongs to the EARLINET special issue. So lidar is most important, and we want to start with lidar. Without lidar, the record-breaking stratospheric event cannot be resolved, cannot be quantified. All the other observations are complementary, but of course very useful and provide the full and consistent picture on temporal and inter-continental scales.***

Page 4, lines 21-24. Temperature and pressure profiles needed for the Fernald method were obtained from GDAS. Is there any radiosounding station nearby? Can you quantify the uncertainty introduced by GDAS profiles instead of using actual radiosoundings?

***Radiosondes are good, but they are only available at certain times. Radiosondes are usually 50-200 km away from the lidar sites. On the other hand, GDAS meteorological fields assimilate all available radiosondes and provide temperature and pressure profiles with a resolution of 1 h and nearest GDAS grid point is usually 20-30 km away from the lidar site. So, meanwhile we believe in GDAS data and prefer to use GDAS profiles in the lidar data analysis. We discuss this aspect now in Sect.2.1.***

***For this specific event (22 August, evening observations) we used Lindenberg radiosonde and GDAS temperature and pressure profiles, the difference (in the extinction profiles) was almost not visible (3% difference, we mention it in Sect 2.1).***

Page 4, lines 26-31. Volume linear depolarization ratio is defined here and used in this paper. I am wondering why this quantity, which simultaneously provides information of particles and molecules, is preferred instead the particle linear depolarization ratio, which provided information on particles solely.

***We use the volume linear depol ratio in Fig.2 (color plot) to identify the stratospheric layer containing mainly irregularly shaped soot particles. The volume depol ratio is easily obtained from the measured signal profiles. Of course, for detailed analysis, we prefer the particle linear depol ratio. But then, the profile of the particle backscatter coefficient has to be computed first, and in the next step, the particle depol ratio can be computed. This is done in paper #2. So, color plots for the particle depol ratio are not so easily obtained, and may contain a lot of uncertainties. Better stay with the color plots for the ‘robust’ volume linear depolarization ratio.***

Page 6, line 15. Here it is stated that the stratospheric smoke particles detected were irregularly shaped. Is it possible to identify the process/processes leading to this kind of shapes using solely your lidar information? Authors refer to the work Haarig et al. (2018). However it would be nice to include some information here.

***We describe the process in the new section 4 (Discussion). Pyrocumulonimbus convection lifts the smoke within an hour into the stratosphere after Rosenfeld et al. (2007). Most of the smoke is not involved in cloud drop nucleation and will directly reach the stratosphere without any chance to interact with trace gas, aerosol particles and cloud drops. So the fire particles (soot particles) preserve their original shape, and the literature shows us that these soot particles are not spherical and can show complicated shape structures.***

Figure 7. Which are the error bars associated to these profiles?

***We avoid to show error bars, just to avoid to overload the figures. The uncertainties in the extinction profiles are almost linearly connected to the uncertainty in the assumed lidar ratio. We measured lidar ratios around 70 sr, and if the lidar ratio varies from 60 to 80 sr, the uncertainty in the extinction profiles is about 15%. We mention this uncertainty in the figure captions of the figures with extinction profiles (Figs. 4 and 6 and also in Sect.2.1, description of the lidar data analysis).***

Page 8, line 25: Here you present results on particle linear depolarization ratio. However, this quantity has not been defined previously.

***We moved the respective figures and discussions to paper #2.***

Technical corrections:

Page 4, line20: replace “was highest” by “was the highest.” Review the entire profile to correct for this typo.

**Done**

Page 4, line 26: replace “volume depolarization ratio” by “linear volume depolarization ratio”. Check the entire body text for replacement.

***Agree! ... but we use volume linear depolarization ratio (similar to particle linear depolarization ratio) as it is used in the EARLINET community...***

Page 6, line 25: replace “Figures” by “Figure”

**Done**

Page 8, line 20: replace “Americian” by “American”

***The discussion of the size distribution part (page 8, lines 19-34) is now in paper #2.***

**Reviewer #2:**

The paper by Albert Ansmann and coauthors documents a record-breaking observation of smoke aerosols above Germany and Czech Republic. The results reported in the Part 1 are based on active and passive remote sensing of aerosol properties using respectively two EARLINET lidars (Leipzig and Kosetice) and two AERONET photometers (Leipzig and Lindenberg). MODIS space-borne observations are used to illustrate the geography of Canadian fires and to provide support for the ground-based observations. The main outcome of the study is based on 3 days of observations and provides estimates of peak extinction coefficient, aerosol optical depth/thickness (AOT), particle mass concentration and accumulation mode effective radius.

The impact of biomass burning and associated pyroconvection on the stratospheric aerosol load is well known. However observational evidence of smoke aerosols in the stratosphere is rare and therefore valuable. The estimates of the smoke plume’s optical and microphysical properties reported in the paper are potentially useful for constraining the models, as suggested in the Introduction. The Canadian wildfires during summer 2017 did indeed have an outstanding impact on the stratospheric aerosol and the presented high-quality observations should be documented in the peer-reviewed literature. However, I believe that the study would make a stronger point had it been consolidated with Part 2.

***See our argumentation above (at the beginning of this reply letter). There are so many new findings, spectacular results, and unique new measurement approaches that it is impossible to combine so many different measurements and observations showing completely different aspects of this event into a single paper. But, we got the message of the reviewer, and improved significantly paper #1 (see the general remarks in the beginning of this reply letter).***

Further, the scientific value of this observational study could be much enhanced, if the authors discuss more carefully their observation in the context of other outstanding aerosol events at northern midlatitudes. The comparison of stratospheric impact of the Canadian smoke event with that of Pinatubo tropical eruption is not totally appropriate as explained below. With that, comparisons with midlatitude eruptions and other biomass burning events are totally missing. I suggest that the authors invest an effort towards enhancing the scientific value of this study through consideration of the following remarks.

***We agree and followed the suggestion. We introduced section 4 (Discussion) and Table 1 with characteristic numbers (max extinction coefficient, max AOT, duration of the event, depth or top height of the stratospheric aerosol layer) for major and moderate volcanic eruptions, and extreme and more typical pyroCB smoke events. We discuss the differences.***

General remarks.

\*It appears that the key statement of this study (as well as of companion paper) is that the observed extinction values were 20 times higher than after Pinatubo. To the casual reader this may suggest that the impact of these fires on stratospheric aerosol is actually much larger than that from the Pinatubo eruption. While this statement is simply misleading, the comparison as such is not correct either. The authors compare peak extinctions of a fresh and compact patch of smoke with that of an older well-mixed volcanic plume spreading over a wide range of altitudes as it was observed by lidars above Europe in 1991-1992. A direct comparison of plumes' optical properties would be justified had a Pinatubo-sized eruption occurred at northern midlatitudes. I believe that before pointing out the superiority of the Canadian smoke peak extinction and AOD over those of Pinatubo, the authors should carefully discuss the aerosol source locations (upwind at midlatitudes versus tropics) and aerosol transport processes (fast zonal transport within LS jet versus slower meridional exchange and mixing). The temporal extents of the observed stratospheric perturbation due to fires (presented observations cover a few days only) and Pinatubo (several years) should also be discussed. Finally, it would be more pertinent to compare the stratospheric AOD (0.6 vs 0.2-0.3) and not the peak extinctions.

***We agree, and introduced Section 4 (Discussion), and discuss all the points mentioned above. We also made an attempt to estimate the maximum Pinatubo effect by looking at lidar data (at Hawaii, DeFoor et al., Barners et al.) and latest global model simulations of Shallcross et al. (these simulation are closely linked to all available lidar observations). The introduced new Table 1 forced us to check all the relevant literature given in the Table.***

\* I am not sure to understand the reasoning for separating this study in two parts. Both parts are centered around lidar soundings and both of them incorporate collocated or nearby AERONET measurements. The distinction seems to be made on the retrieved parameters, e.g. volume particle size distributions in part 1 and mass distribution in Part 2. I think the reader would much appreciate having all the parameters from a time-limited observation in a single article.

***We got the message, but please see our argumentation at the beginning of this reply letter. Our mistake was to select almost the same title for both papers and also that we wanted to have a compact set of two papers which are closely related to each other. Now we separated all results, there is almost no overlap between the two papers, and both papers will show up as stand-alone papers with new and unique results worthwhile to be published. I hope this is acceptable!***

\* The structural organization of the article should be reconsidered. The introduction appears too lengthy, whereas the discussion section is totally missing. I suggest to introduce the discussion section, which would include some parts of the Introduction and a careful stipulation regarding smoke vs Pinatubo comparison. Section 3 (observations) would be much easier to follow had it been structured by the observation sources.

***This comment triggered a lot. We introduced the requested discussion section (Sect. 4) and Table 1, and also improved the structure of Sect. 3 (observations) by having six subsections (3.1 overview MODIS OMI from Canada to Europe, 3.2 Overview lidar, 21-23 August, aerosol layering, 3.3 source identification, 3.4 lidar profiles, central Europe, three stations, 3.5 AERONET AOT Leipzig and bias discussion, 3.6 MODIS Leipzig area). In subsection 3.5, we have a new Table 2, showing the AERONET AOT vs lidarAOT bias.***

\* Coming back to the extreme extinction and AOD observed by Leipzig lidar. While there is no reason to question the data, I wonder if similar levels of aerosol abundance were observed by the neighboring lidars stations, e.g. Cabauw, Garmish, Hohenpeisenberg, etc. And what is truly puzzling is why the authors do not compare the extinction from two Polly lidars that operated in close vicinity. Is it possible to invert the Kosetice 532 nm data and present the time curtain of extinction rather than attenuated backscatter?

*We added the EARLINET station of Hohenpeissenberg (the German Weather Service has a continuously running Polly lidar), we checked Cabauw and Garmisch, but they have (almost) no data for this time period. The good agreement between the Hohenpeissenberg, Leipzig, and Kosetice observations (especially for the 22 August, see new Fig.4) was surprising. At all three stations, the maximum extinction coefficient was close to 500 Mm<sup>-1</sup>.*

*We avoid to convert the attenuated backscatter! The attenuated backscatter is easily obtained (range corrected signal at 1064 nm) and nicely shows the evolution of the aerosol layers. If we show the color plot in terms of extinction, the reader may argue that it introduces the high rate of uncertainty. The lidar ratio can be very different in the PBL, free troposphere and stratosphere. Nevertheless, we decided to provide some essential numbers (extinction values) for the pronounced stratospheric and tropospheric structures and layers we found. That is sufficient and helps, we believe.*

Specific remarks

P.3, The second paragraph should belong to the discussion section

*The introduction is completely rewritten and shortened. It is now more compact and straightforward. The second paragraph is removed.*

P.4, 1.6. Typo in Leipzig longitude

*Changed*

P.5, 1.30. “Similar indications : : : were observable: : :” An appropriate reference is missing here.

*This part is removed.*

P.6, 1.5. “Figure 3 provides an overview of aerosol layering over Central Europe: : :” To me this is an example rather than an overview.

*We completely agree with the reviewer. We changed the text accordingly.*

P.6, 1.20-22. Why mention global (general?) circulation models here? HYSPLIT is a Lagrangian trajectory model. Also, how does the pyrocumulonimbus convection influence the long-range transport? I think, the caveats of trajectory analysis for smoke tracking should be explained more carefully.

*Unfortunately, we cannot do that. We are not experts for atmospheric modeling (including the HYSPLIT tool). We can show convincing air flow pattern, fortunately for us, but more is not possible. The only trustworthy way to identify the sources of the forest fire smoke is, to our opinion, tracking of aerosol fields by means of satellite data (MODIS, AOT, OMI-AI, OMPS-UVAI) from the fire areas to the lidar sites. We did this in Sect. 3.3: We combined the satellite aerosol features (with rather strong AI) over northern Canada with forward HYSPLIT modeling. Here, we use day-by-day OMPS UVAI maps provided by Khaykin et al. (2018). More details below and in the revised version (see Sect. 3.3).*

*At the end, we found a clear link between the extreme (record-breaking) pyroCB event over southern and central British Columbia on 12 August 2017 and the record-breaking smoke event over central Europe (21-22 August 2017).*

P.6, l.23. “: : at tropospheric as well as stratospheric height: : :”. The highest-level trajectory is initialized at 12000 m, which is just around the tropopause on 21 August. The smoke was observed as high as 15-16 km above Kosetice so it would be useful to show trajectories initialized at higher levels.

***We decided not to show backward trajectories for heights of 15-16 km height. Khaykin et al. (2018) pointed out that the smoke layers ascended by 2-3km per day (cross isentropic transport) during the first 2 days when the AOT was certainly of the order of >2 or even 3 ... probably by the self-lifting effect (triggered by strong absorption of solar radiation). And this aspect is not covered by HYSPLIT, we believe.***

***So, we did not change the trajectory figure (now Fig.3). The main message of the HYSPLIT backward trajectories is: Yes, the smoke-containing air masses we observed at the beginning of the record-breaking episode, 21 August (20 UTC) at heights of 6, 9, and 12 km height above Kosetice originated from North America, roughly from the region of western Canada 10 days before. We are happy that HYSPLIT was able to produce this convincing airflow.***

P.7, l.33-34. Here the authors refer to the period of smoke observation by the instruments involved in this study either as the “smoke period” or “smoke event”. Such a terminology is not quite correct because the actual period when the smoke was observed above Europe and elsewhere in NH spanned several months.

***I hope we have now a better definition and more correct terminology. At least we clearly say that we focus on the ‘event’ or episode which began over the Czech lidar station (Kosetice) on 21 August, 15UTC, and ended on 23 August, 5 UTC. The clear onset and the abrupt end of the record-breaking is another indication that this smoke layer must have something to do with a temporally well-defined meteorological process (like a thunderstorm). Continuous bush fires would probably lead to more continuous structures in the observed stratospheric aerosol structures. This aspect is also mentioned in Sect.3.3.***

Figure 1. MODIS detected powerful wildfires at different locations across Canada, particularly in British Columbia and Northwest territories. Which cluster of fires has caused the extreme levels of smoke in the stratosphere? Could anything be inferred from trajectory analysis?

***Just to repeat our statements: In section 3.3 (source identification) we explain how we identified the source region (central and southern British Columbia). We used the day-by-day satellite UVAI maps in the Khaykin et al., (2018) paper (14-24 August 2017) and HYSPLIT forward trajectories. We started these trajectories on the afternoon of 12 August when rather strong thunderstorms occurred and formed the strongest pyrocumulonimbus complex ever observed. There is a clear match between these 12 August forward trajectories and areas with rather high UVAI over northern Canada. And these UVAI fields moved then across the Atlantic towards Europe during the next 10 days and one the branches finally crossed central Europe.***

Figure 2. The photos serve a nice illustration of the stratospheric smoke. However, in order to place them in a scientific context, one should at least provide the azimuthal direction at which these photos were taken.

***We removed the figure***

Figure 3. The plot could be much improved by adding the tropopause height curve (or perhaps even a drawn line). This would help distinguishing tropospheric and stratospheric smoke plumes.

***Is now improved, white lines show the tropopause in both plots.***

## **Juan- Carlos Antuna:**

### General Comments:

The article address a relevant scientific question: the scarce measurements of stratospheric aerosols produced by big wildfire events. The particular event discussed is reported to be the one producing the biggest Aerosol Optical Thickness (AOT) among all the already measured. The measurements from multiple instruments show a noticeable contribution to both the tropospheric and stratospheric aerosols over Europa after its transport from the wildfires region in Canada. The article present novel data measurements but fall short in deriving substantial conclusions. Apart from novelty of the measurements, very few science and discussions is contributed, with the promise to do it in the second part.

***I hope we can convince Juan Carlos that our revised paper was improved significantly. He pushed us forward. Thank you for this! We can say that the paper was largely modified and many parts were re-written, many new aspects, results, interpretations, and comparisons (Table 1, comparison of volcanic and smoke events) are included in the revised version of paper #1. On the other hand side, to our opinion the fact that we observed a record-breaking stratospheric contamination should be justification enough to publish this observation. We totally agree that papers should contribute to science (better understanding of atmospheric processes), but there must be also room for reporting and documenting spectacular, record-breaking and thus historical events using ground monitoring measurements and space-based observations.***

The reviewer's opinion is that the authors have two options: They may combine parts 1 and 2 of the article in one paper or part 1 may be improved and modified considerable. It could be suitable, for example, as an article on Atmospheric Measurement Technique demonstrating how to assemble a set of valuable measurements, including more discussion on the results and highlighting the synergy between the measurements to provide a detailed characterization of stratospheric aerosols originated by wildfire smoke. A detailed discussion will be necessary about the advantages/disadvantages of each instrument with respect to the rest.

***So, we choose the option: improve and modify paper #1 considerably. A discussion on the synergy of different observations, advantages and disadvantages is however not given. We think that it is obvious that many different and complementary observations are always useful. Without different observations the discussion is usually not convincing and trustworthy. It is also obvious that lidar is needed. Otherwise it is impossible the obtain a clear picture of the stratospheric perturbation.***

***We only compare AERONET with lidar results to conclude that AERONET underestimates the AOT at these very unusual conditions with dense aerosol layers in 10 to 17 km distance from the photometer (with receiver full angle of 1.2°, 20 mrad) because of strong forward scattering of sunlight (see Sect. 3.5 and new Table 2 for more details).***

### Specific Comments :

The abstract is clear and describe correctly the limited content of the article.

Page 2, line 6: replace "heterogenous" by "heterogeneous"

***We replace all 'heterogenous' in the text.... Now heterogeneous***

Page 3, line 23: replace "ballon" by "balloon"

***We replaced all 'ballon' in the text.... Now balloon...***

Page 4, line 29: replace "shperical" by "spherical"

***Improved throughout the text***

Page 10, line 2: replace “Februray” by “February”

***Improved throughout the text***

The revised version of paper #1 is attached (see next pages)

# Extreme levels of Canadian wildfire smoke in the stratosphere over central Europe on 21–22 August 2017

Albert Ansmann<sup>1</sup>, Holger Baars<sup>1</sup>, Alexandra Chudnovsky<sup>2</sup>, Ina Mattis<sup>3</sup>, Igor Veselovskii<sup>4</sup>, Moritz Haarig<sup>1</sup>, Patric Seifert<sup>1</sup>, Ronny Engelmann<sup>1</sup>, and Ulla Wandinger<sup>1</sup>

<sup>1</sup>Leibniz Institute for Tropospheric Research, Leipzig, Germany

<sup>2</sup>Tel Aviv University, Porter School of Earth Sciences and Environment, Tel Aviv, Israel

<sup>3</sup>Observatory Hohenpeissenberg, German Weather Service, Hohenpeissenberg, Germany

<sup>4</sup>Physics Instrumentation Center of General Physics Institute, Moscow, Russia

*Correspondence to:* A. Ansmann  
(albert@tropos.de)

**Abstract.** Light extinction coefficients of  $500 \text{ Mm}^{-1}$ , about 20 times higher than after the Pinatubo volcanic eruptions in 1991, were observed with European Aerosol Research Lidar Network (EARLINET) lidars in the stratosphere over central Europe on 21–22 August 2017. Pronounced smoke layers of 1–2 km vertical extent were found 2–5 km above the local tropopause. Optically dense layers of Canadian wildfire smoke reached central Europe 10 days after injection into the upper troposphere and lower stratosphere caused by rather strong pyrocumulonimbus activity over western Canada. The smoke-related aerosol optical thickness (AOT) was close to 1.0 at 532 nm over Leipzig during the noon hours on 22 August 2017. Smoke particles were found throughout the free troposphere (AOT of 0.3) and in the pronounced 2–km thick stratospheric smoke layer between 14 and 16 km height (AOT of 0.6). The lidar observations indicated peak mass concentrations of  $70\text{--}100 \mu\text{g m}^{-3}$  in the stratosphere. Besides the lidar profiles, we analyzed Moderate Resolution Imaging Spectroradiometer (MODIS) fire radiative power (FRP) over Canada, and the distribution of MODIS AOT and Ozone Monitoring Instrument (OMI) Aerosol Index across the North Atlantic, showing similar pattern and a clear link between the western Canadian fires and the aerosol load over Europe. We present Aerosol Robotic Network (AERONET) sun photometer observations, compare photometer and lidar-derived AOT, and discuss an obvious bias (too low smoke AOT) in the photometer observations. MODIS AOT for the Leipzig area confirm the high smoke AOT values derived from the lidar measurements. We finally compare the strength of this record-breaking smoke event (in terms of particle extinction coefficient and AOT) with major and moderate volcanic events observed over northern midlatitudes.

## 1 Introduction

Exceptionally dense Canadian wildfire smoke layers causing an aerosol optical thickness (AOT) close to 1.0 at 532 nm crossed central Europe between 3 and 16 km height on 21–22 August 2017. Stratospheric light-extinction coefficients observed at 14–16 km height, about 3–4 km above the local tropopause, were 20 times higher than the maximum extinction values observed in the stratosphere over central Europe in the winters of 1991 and 1992 after the strong Mt. Pinatubo eruption in June 1991

(Ansmann et al., 1997; Jäger, 2005). We never observed such a strong perturbation of stratospheric aerosol conditions with our lidars before and document this record-breaking event in this article. North-American aerosol signatures are usually detected in the height range from 3–8 km over central Europe during the summer seasons (Mattis et al., 2003, 2008) with AOTs of 0.02–0.05, and only in very few cases, enhanced smoke-related extinction coefficients were observed just above the tropopause.

5 Table 1 gives an overview of extreme and moderate events of stratospheric perturbations (related to volcanic eruptions and wildfire periods) and corroborates the extraordinarily heavy contamination of the lower stratosphere over central Europe on 21–22 August 2017 (more details in Sect. 4).

Record-breaking intensive fires combined with the formation of exceptionally strong and well organized pyrocumulonimbus clusters in western Canada (<https://visibleearth.nasa.gov/view.php?id=90759>, [https://earthdata.nasa.gov/fire-and-smoke-](https://earthdata.nasa.gov/fire-and-smoke-in-canada)  
10 [in-canada](https://earthdata.nasa.gov/fire-and-smoke-in-canada)) were responsible for these unprecedentedly optically thick stratospheric smoke layers reaching Europe. Fromm et al. (2000, 2003) and Rosenfeld et al. (2007) showed that large amounts of fire smoke can be lifted up to the tropopause within a short time period of less than an hour and partly reach the lower stratosphere via the formation of pyrocumulonimbus clouds which are associated with strong updrafts with vertical wind velocities of 10-30 m/s (Fromm et al., 2010; Peterson et al., 2017). Self-lifting effects (Boers et al., 2010; Siddaway and Petelina, 2011; de Laat et al., 2012) and gravito-photophoresis  
15 forces (Rohatschek, 1996; Pueschel et al., 2000; Cheremisin et al., 2005; Renard et al., 2008) lead to a further ascent of the soot-containing layers.

The 2017 wildfire season (April-September) was the worst ever burning season in British Columbia, Canada, since recording began in 1950 (<https://globalnews.ca/news/3675434/2017-officially-b-c-s-worst-ever-wildfire-season/>) and exceeds even the year 1958 (855000 ha area burned) with about 900000 ha of burned forest. Recent studies suggest a direct link between  
20 increasing fire activity in northwestern United States and Canada and changing climate and weather conditions (Liu et al., 2009, 2014; Kitzberger et al., 2017). The summer half year of 2017 was unusually dry in western Canada and helped to create a hot, dry environment with a large reservoir of underbrush which is favorable burning material.

According to spaceborne CALIPSO (Cloud-Aerosol Lidar and Infrared Pathfinder Satellite Observation) lidar observations presented by Khaykin et al. (2018) the fire aerosol traveled eastward after entering the upper troposphere and lower strato-  
25 sphere, crossed the North Atlantic, Europe, northern Asia, and circled around the globe within less than 20 days. Khaykin et al. (2018) further pointed out that the optically dense smoke plumes obviously ascended by about 2-3 km per day during the first days after injection into the upper troposphere and lower stratosphere. The smoke layers were observed all over Europe with ground-based lidar systems of the European Aerosol Research Lidar Network (EARLINET) (Pappalardo et al., 2014) and further lidars operated in a long-term mode (Khaykin et al., 2018). Traces of stratospheric smoke were continuously detected  
30 over Europe until the end of 2017.

Large volcanic eruptions were considered for a long time to be the only process by which significant amounts of aerosols and gases can abruptly enter the lower stratosphere. Pyrocumulonimbus-related smoke injections as reported here may foster the discussion on the role and relevance of alternative path ways of massive perturbations of stratospheric aerosol conditions. The extreme August 2017 fire period provides an ideal opportunity to test atmospheric transport models regarding smoke  
35 long-range transport, spread, and removal and the direct and indirect impact of the soot layers on climate. Volcanic and smoke

aerosols show very different chemical, physical and morphological characteristics. In contrast to the liquid and thus spherical sulfuric acid droplets of volcanic origin, stratospheric soot particles are solid, non-spherical, significantly absorb solar radiation, and can ascent to greater heights. Soot particles influence the evolution of ice clouds by serving as ice-nucleating particles in heterogeneous (deposition) freezing processes (Hoose and Möhler, 2012), whereas liquid sulfuric acid droplets influence cirrus occurrence and evolution via homogeneous ice nucleation (Jensen and Toon, 1992; Sassen et al., 1995; Liu and Penner, 2002). The complex transport features and climatic influences of stratospheric soot layers make it necessary to compare simulated smoke scenarios and the evolution of the smoke layer during long-range transport with available observations. Recent advances in ground-based and spaceborne active and passive remote sensing and thus the availability of a dense set of observations of the biomass burning material will allow detailed model validation studies.

The article is organized as follows: Data analysis and product information are provided next. In Sect. 3 (observations), we begin with an overview of the fire situation in western Canada in August 2017 and the transport of smoke across the Atlantic towards Europe based on Moderate Resolution Imaging Spectroradiometer (MODIS) and Ozone Monitoring Instrument (OMI) measurements. Next, the lidar observations performed from 21-23 August 2017 (episode with maximum stratospheric pollution) are presented. Smoke observations at three lidar stations in central Europe (Leipzig, Hohenpeissenberg near Munich, and Kosetice near Prague) are shown. Aerosol Robotic Network (AERONET) observations in central Europe and MODIS AOT values around the Leipzig EARLINET/AERONET station will complement the documentation of the extraordinarily strong wildfire smoke event.

## 2 Instruments, data analysis, and products

### 2.1 Lidar data analysis

Three aerosol lidars of the Polly (*Portable lidar system*) type (Althausen et al., 2009; Engelmann et al., 2016; Baars et al., 2016) were run at the Leipzig EARLINET station (51.3°N, 12.4°E, 110 m a.s.l., Leibniz Institute for Tropospheric Research, TROPOS), at the Hohenpeissenberg EARLINET station (47.8°N, 11.0°E, 1000 m a.s.l., Meteorological Observatory Hohenpeissenberg, German Weather Service), about 60 km southwest of Munich, and at Kosetice (49.6°N, 15.1°E, 500 m a.s.l.), Czech Republic. A triple-wavelength Polly was operated by TROPOS at Kosetice, 75 km southeast of Prague and about 275 km southeast of Leipzig, for three months in the framework of an aerosol field campaign lasting from July to October 2017. During the smoke event northwesterly winds prevailed in the stratosphere and the air masses crossed Leipzig about 3–4 hours before reaching Kosetice.

The so-called Fernald method (Fernald, 1984) was used to derive height profiles of particle extinction coefficient from the lidar observations at daytime. The reference height was set around 10–11 km height (tropopause region). The particle extinction-to-backscatter ratio (lidar ratio) is needed as input. We used a value of 70 sr for 532 nm. This lidar ratio of 70 sr was measured with our Raman lidars after sunset on 22 August 2017 (Haarig et al., 2018). An uncertainty of the obtained extinction profile is almost directly dependent on the lidar ratio uncertainty. 15% uncertainty in the lidar ratio input parameter (assuming variations of 10 sr around 70 sr) thus leads to a relative uncertainty of about 15% in the smoke extinction values.

To reduce the influence of signal noise the signal profiles have to be smoothed. We used vertical gliding-averaging window length of 185 m in the boundary layer (up to 2.5 km height) and 750 m (above the boundary layer up to 16 km height). The sensitivity tests with different smoothing lengths of 175 m, 350 m, and 750 m in the free troposphere revealed that the main layering features are well resolved by using the comparably large vertical window length of 750 m. The large smoothing length was necessary because the densest smoke layers crossed the lidar at Leipzig during the noon hours when the signal noise by sunlight was the highest.

Temperature and pressure profiles are required in the lidar data analysis to correct for Rayleigh extinction and backscattering. This information is taken from the GDAS (Global Data Assimilation System) data base which contains profiles of temperature and pressure from the National Weather Service's National Centers for Environmental Prediction (NCEP) (GDAS, 2018) with a horizontal resolution of  $1^\circ$ . We ignore a minor ozone absorption effect at 532 and 607 nm in the determination of smoke extinction coefficient and thus an additional uncertainty of few percent. Alternatively to the GDAS profiles, we selected nearby radiosonde temperature and pressure profiles (Munich, Prague, Lindenberg) in the extinction profile retrieval to check the impact of potential temperature and pressure uncertainties on the results and found rather small deviations between the different particle extinction profiles (of  $<3\%$  for 22 August 2017). However, one should emphasize that the GDAS data set is based on all available radiosonde observations (in central Europe). The radiosonde profiles are assimilated into the atmospheric model so that the GDAS data (providing temperature and pressure profiles every 3 hours and for distances of typically 20-30 km to the lidar stations) are more representative for the actual meteorological conditions over the lidar sites than the few radiosonde profiles providing the meteorological state for regions typically 60-180 km away from the lidar site and for fixed times (usually for 0 and 12 UTC) and thus coarse temporal resolution.

In Sect. 3, we will also show height-time displays of the volume linear depolarization ratio. This quantity is defined as the ratio of cross-to-co-polarized backscatter coefficient.  $C_o$  and cross denote the planes of polarization (for which the receiver channels are sensitive) parallel and orthogonal to the plane of linear polarization of the transmitted laser pulses, respectively. The volume linear depolarization ratio is easily obtained from the lidar raw signals and enables us to identify non-spherical particles such as ice crystals and irregularly shaped smoke particles. The depolarization ratio is comparably high when the particles are non-spherical and very low (almost zero) if the particles are spherical (sulfuric acid droplets, soot particles with a liquid shell).

## 2.2 AERONET products

The EARLINET stations at Leipzig and Hohenpeissenberg are collocated with an Aerosol Robotic Network site (Holben et al., 1998). For comparison of the Kosetice lidar observations with respective AERONET measurements we used the data collected at the AERONET Brno site, which is 115 km southeast of Kosetice (and thus downwind of the lidar site at 14–16 km height on 21–22 August 2018). The AERONET sun/sky photometer measures AOT at eight wavelengths from 339 to 1638 nm (AERONET, 2018). Sky radiance observations at four wavelengths complete the AERONET observations. From the spectral AOT distribution for the wavelength range from 440 to 870 nm the wavelength dependence of AOT expressed in terms of the Ångström exponent AE is obtained. Furthermore, the 500 nm fine mode fraction FMF (fraction of 500 nm fine-mode AOT to

total AOT), and particle size distribution for the entire vertical column is derived (O'Neill et al., 2003; Dubovik et al., 2006). Fine mode particles have per definition a diameter of  $\leq 1 \mu\text{m}$ .

### 2.3 Satellite-derived products: MODIS and OMI retrievals

Next, we analyzed spatial and temporal pattern of MODIS AOT, MODIS-derived fire radiative power (FRP), and Ozone Monitoring Instrument (OMI) Aerosol Index (AI, 354 nm) observed over the area that covers Western Canada and extends to Europe in August 2017. MODIS AOT values (at 550 nm) were generated by using the GES-DISC Interactive Online Visualization and analysis Infrastructure (GIOVANNI) developed by the National Aeronautics and Space Administration (NASA) Goddard Earth Sciences (GES) Data and Information Services Center (DISC) (Acker and Leptoukh, 2007; Berrick et al., 2009). GIOVANNI provides Level 3 (e.g.,  $1^\circ$  spatial resolution pixel size) product that is aggregated and averaged from the Level 2 product (e.g.,  $0.1^\circ$  resolution pixel size).

OMI AI for the entire August 2017 period were also produced with GIOVANNI. Positive values of AI are associated with UV absorbing aerosols, mainly mineral dust, smoke and volcanic aerosols. Negative values of AI are associated with non-absorbing aerosols (for example sulfate and sea-salt particles) from both natural and anthropogenic sources (Torres et al., 1998; Buchard et al., 2015; Hammer et al., 2016). Values near zero indicate cloud fields.

The FRP product enables distinction between fires of different strengths at 1 km resolution using Terra and Aqua satellites (Ichoku et al., 2008). Instantaneous FRP values range between 0.02 MW and 1866 MW per  $1 \text{ km} \times 1 \text{ km}$  pixel, with global daily means ranging between 20 and 40 MW (Ichoku et al., 2008). As shown recently by Freeborn et al. (2014), MODIS FRP have an uncertainty of 26.6% at the 1 sigma level. We used active fire products from the MODIS (MCD14DL product) in shapefile formats (<https://earthdata.nasa.gov/earth-observation-data/near-real-time/firms/active-fire-data>). Only high quality FRP values above 50 MW (and exceeding accuracy levels  $>65\%$ ) were mapped.

Finally, we used 550 nm AOT images for the Leipzig region for 22 August 2017 obtained with the MODIS combined DT (dark target) and DB (deep blue) algorithms (Remer et al., 2013). The most recently released MODIS Collection 6 product MOD04\_3K (for Terra) and MYD04\_3K (for Aqua) contains AOT at a 3 km horizontal resolution in addition to the L2 10 km product (Remer et al., 2013; Levy et al., 2015). The retrieval algorithm of the higher resolution product is similar to that of the 10 km standard product with several exceptions (for more details, see [http://modisatmos.gsfc.nasa.gov/MOD04\\_L2](http://modisatmos.gsfc.nasa.gov/MOD04_L2)). Validation against surface sun photometer shows that two-thirds of the 3 km retrievals fall within the expected error on a regional comparison but with a high bias of 0.06 especially over urban surfaces. The uncertainty in the retrieved AOT is  $0.05 \pm 0.15 \times \text{AOT}$  for  $\text{AOT} \leq 1.0$  (Levy et al., 2010, 2013). In this study, we use the MODIS Collection 6 (C006) AOT retrievals at  $3 \text{ km} \times 3 \text{ km}$  (at nadir) spatial resolution collected with Terra (10:30 local equatorial crossing time) and Aqua (13:30 local equatorial crossing time) over Leipzig on 22 August 2017 (MODIS, 2018). In addition, we also used Sentinel-2 multi-spectral instrument (MSI) RGB (red green blue) image collected on August 22 to get the cloud cover and ground conditions over Leipzig.

### 3 Observations

#### 3.1 Overview: The smoke situation in August 2017 as seen with MODIS and OMI

Figure 1 shows the distribution of fire clusters all over Canada in August 2017 obtained from MODIS observations together with maps of the 354 nm Aerosol Index (OMI) and MODIS-derived 550 nm AOT for the main corridor of smoke transport across the North Atlantic towards Europe. The number of fire pixels with FRP >50 MW (for 1 km × 1 km pixels) was of the order of 10000 in August 2017. The fire activity was highest in British Columbia.

Figures 1b and c show enhanced values of OMI 354 nm AI and MODIS 550 nm AOT (August 2017 mean values) over the entire region from western Canada to Europe. The spatial features of fire clusters over western Canada match the elevated AOT and AI values over this region. Furthermore, as also evident from Fig. 1, both satellite systems (MODIS, OMI) independently show similar results (pattern) in terms of AI and AOT. The smoke which crossed central Europe on 21–22 August 2017 originated from the most western part of Canada. The source identification aspect is discussed in more detail in Sect. 3.3.

Note that the shown AOT is composed of contributions from aerosol particles in the planetary boundary layer (PBL, about 0.05 over the Atlantic and 0.1–0.3 over the continents), from smoke and anthropogenic haze in the free troposphere (FT, about 0.05–0.25), and from the smoke particles in the stratosphere (S). Tropospheric 550 nm AOT thus ranges from about 0.05 to 0.5 which makes the interpretation of the satellite-based AOT and AI maps concerning the stratospheric aerosol load difficult. The August 2017 mean anthropogenic and marine AOT contribution may have been of the order of 0.1–0.3 at 550 nm. Thus, smoke dominated the AOT pattern in August 2017. Frequently the AOT values exceeded 0.5.

A clear sign for the presence of absorbing wildfire smoke particles are the high AI values. AI frequently exceeded 1.0 and indicates a strongly absorbing aerosol. The impact of anthropogenic haze and marine particles to absorption of radiation at 354 nm is comparably low. AI typically ranges from -0.5 and 0.2 over North America and Europe in the absence of biomass burning (Hammer et al., 2018).

#### 3.2 The 21–23 August 2017 smoke event over central Europe

Figure 2 shows the aerosol layering over Kosetice, Czech Republic, from 20–23 August 2017. Coherent smoke structures were observed in the troposphere as well as in the stratosphere over more than one day. Unfortunately, clouds at 1–4 km height disturbed aerosol and cloud profiling considerably during the daytime periods. The tropopause height (indicated as white lines in Fig. 2) was mainly between 10 and 11.5 km from 20–23 August. The extreme event with particle extinction coefficients mostly from 250–500  $\text{Mm}^{-1}$  in the lower stratospheric layer lasted from 21 August, 15:00 UTC until 23 August, 5:00 UTC. In the beginning, the 2-km thick smoke layer was detected at 12 km height and at the end at 15–16 km height. Particle extinction coefficients in the free troposphere (between 2–7 km height) were about 20–50  $\text{Mm}^{-1}$  on 21–23 August as we will discuss in more detail in Sect. 3.4.

The apparently ascending stratospheric soot layer (observed from 21–23 August) is the results of two different influences. Khaykin et al. (2018) found that the smoke plumes ascended rapidly over the first few days after injection into the upper troposphere with a rate of 2–3 km per day. This cross isentropic ascent was caused by radiative heating of smoke aerosols

(Boers et al., 2010). On the other hand side, the wind velocity decreased with height from the tropopause to 16 km height (GDAS, 2018) as well as from the tropopause to the middle troposphere (5 km height). Caused by the higher velocities in the tropopause region, here first layers crossed the lidar site. The plumes in the middle troposphere and in the stratosphere at 15-16 km height arrived over Kosetice one day later. According to the Prague radiosonde launched on 22 August 12 UTC and 5 23 August 2017, 0 UTC, wind speeds were of the order of 50 m/s at tropopause levels and about 15-20 m/s at 15–16 km height.

The volume linear depolarization ratio, shown in Fig. 2 (bottom), contains information on particle shape. The depolarization ratio is highest in the cirrus clouds (consisting of strongly light-depolarizing hexagonal ice crystals) and is also significantly enhanced in the stratospheric smoke layer caused by irregularly shaped and most probably dry and non-coated soot particles. Observations (including photographs) of stratospheric smoke particles indicate that stratospheric soot particles can be rather irregular in shape (Strawa et al., 1999). The 532 nm volume linear depolarization ratio was mostly between 0.1 and 0.2 at heights 10 from 12–16 km. The relationship between particle shape and particle linear depolarization ratio is discussed in Haarig et al. (2018).

In contrast to stratospheric particles, tropospheric smoke particles are almost spherical so that the volume depolarization ratio is significantly  $<0.1$ . Chemical processing and interaction with particles and trace gases in the troposphere lead to 15 changes of the shape properties of the fire smoke particles. They are partly coated, embedded, or partially encapsulated after long-range transport (China et al., 2015). Smoke particles with a solid soot kernel and a spherical (liquid) sulfuric acid shell (Dahlkötter et al., 2014) would cause a depolarization ratio close to zero.

### 3.3 Identification of the smoke source regions

The HYSPLIT backward trajectories (Stein et al., 2015; Rolph et al., 2017; HYSPLIT, 2018) in Fig. 3 provide an impression 20 of the upper tropospheric air flow between North America and central Europe during the 10 days from 12-21 August 2017. According to the backward trajectories, the smoke traveled about 7–10 days from western Canada to central Europe. This is in good agreement with the travel time derived from the spaceborne CALIPSO lidar observation presented by Khaykin et al. (2018).

To identify the sources regions of the wildfire smoke observed over Europe we inspected HYSPLIT forward trajectories 25 starting over fire region in western Canada. We combined the analysis of forward trajectories with daily maps of OMI AI, MODIS 550 nm AOT and UV Aerosol Index (UVAI) obtained from observations with the spaceborne OPMS (Ozone Mapping and Profiler Suite) as presented in the Supporting Information S2 of Khaykin et al. (2018). Our study was guided by the fact that a rather strong pyrocumulonimbus complex (generated from five thunderstorms) developed over the fire areas in southern-central British Columbia (see B.C. region in Fig. 1) and the northwestern United States in the afternoon of 12 August 2017 30 and lasted about five hours. It was the biggest pyrocumulonimbus event ever observed, the most significant fire-driven thunderstorm event in history (personal communication, David Peterson, U.S. Naval Research Laboratory, Monterey, California, April 2017). This event obviously triggered the formation of an optically thick smoke layer (probably with an AOT of  $>2-3$ ) in the upper troposphere and lower stratosphere over British Columbia. According to the forward HYSPLIT trajectories started over southern-central British Columbia in the afternoon of 12 August 2017 between 5 and 12 km height these dense smoke plumes

traveled northward during the next two days. This is in agreement with the UVAI maps (Khaykin et al., 2018) that show a large region with very high UVAI over northern Canada extending from about 65–75°N and 90–140°W on 14 August 2017 (early afternoon). As further shown in the day-by-day OMPS UVAI maps, the smoke fields then crossed Canada, the Atlantic and split into at least two branches over the eastern Atlantic, and one of these branches crossed central Europe on 21–22 August 2017.

### 3.4 Vertical profiling of smoke

Figure 4 shows the height profiles of particle extinction coefficient at 532 nm as measured over the three Polly lidar sites in southern and central-eastern Germany and Czech Republic on 21–22 August 2017. The locations of the two EARLINET stations at Hohenpeissenberg and Leipzig, and the third one at Kostice are shown in Fig. 5. Maximum extinction coefficients reached  $500 \text{ Mm}^{-1}$  at all three stations. Values of the stratospheric AOT are given Fig. 5. As mentioned in Sect. 2.1, the uncertainty in the particle extinction coefficients and AOT(s) values is almost directly proportional to the uncertainty in the lidar ratio assumption. We used a smoke lidar ratio of 70 sr in the extinction coefficient retrieval (3–17 km height range) as measured with several Raman lidars at Leipzig in the evening of 22 August 2017 (Haarig et al., 2018) and also found over Hohenpeissenberg and Kosetice in the nights from 21–22 August and 22–23 August 2017, respectively. By assuming a realistic smoke lidar ratio from 60–80 sr for 532 nm, the uncertainty in the extinction profiles is of the order of 15%.

The record-breaking smoke event began over Hohenpeissenberg on 21 August (7:00 UTC) and ended on 22 August, 19:00 UTC, and thus occurred 8–10 hours earlier than over Kosetice and 3–5 hours earlier than over Leipzig (upwind of Kosetice). On 21 August, when the first smoke layers arrived over central Europe, the smoke layers were found close to the tropopause. One day later the layers crossed the lidar stations at much greater heights and accumulated in the height range from 14–17 km height, 2–5 km above the local tropopause. These layers traveled with much lower wind speed than the ones at heights close to the tropopause observed one day before. The stratospheric 532 nm AOT in Fig. 5 ranged from 0.37–0.59 during the passage of the densest stratospheric smoke plumes on 21–22 August 2017.

Note that light-extinction coefficients of the order of  $500 \text{ Mm}^{-1}$  indicate an horizontal visibility of around 6 km in 14–16 km height. At these stratospheric heights the visibility is usually several hundreds of kilometers. Peak mass concentrations were of the order of  $70\text{--}100 \mu\text{g m}^{-3}$  in the lower stratosphere over central Europe around noon of 22 August 2017 (Haarig et al., 2018). Particle extinction values close to  $500 \text{ Mm}^{-1}$  in combination with lidar ratios around 70 sr corresponds to backscatter ratios (total-to-Rayleigh backscatter) of up to 25–30 at 532 nm at 15 km height. Khaykin et al. (2018) reported backscatter ratios around 10 (ground-based lidar) and almost 20 (CALIPSO lidar) for measurements over southern France in the second half of August and the first half of September 2017.

Figure 6 shows noon and evening lidar profiles for the entire atmosphere over Leipzig from the ground to 16.2 km height. At noon (11:00–12:00 UTC), the entire free troposphere contained traces of smoke. The 532 nm AOT was 0.3 in the free troposphere and about 0.6 in the stratosphere for the height range from the tropopause up to 16.2 km height. The smoke-related AOT was significantly lower in the evening hours (blue curve) with a free tropospheric contribution of 0.08 and a stratospheric

contribution of 0.2–0.25. The evening measurements at Leipzig (22 August, 20:40–23 UTC) with three polarization/Raman lidars are presented and discussed in Haarig et al. (2018).

The high stratospheric AOT of 0.59 over Leipzig is in good agreement with CALIPSO lidar measurements (Khaykin et al., 2018). The maximum AOT measured with the CALIPSO lidar was of the order of 1.0 at 532 nm. These values occurred over northeastern Canada on 17–19 August 2017 and thus a few days upstream of central Europe. Khaykin et al. (2018) originally reported maximum AOTs of 0.7 only, but these values were directly estimated from the height profiles of the attenuated backscatter coefficients. They were not corrected for particle extinction influences (i.e., attenuation effects). If we take smoke extinction (according to an AOT of the order of 0.7–1.0) in the retrieval into account, the true profile of the particle backscatter coefficient multiplied by a smoke lidar ratio of 70 sr leads to an AOT about a factor of 1.5 higher than the apparent one given by Khaykin et al. (2018) and thus to values of the order of 1.0.

### 3.5 AERONET observations at Leipzig

Figure 7 shows the Leipzig AERONET observations from 21–23 August 2017. Level 2.0 data are presented (AERONET, 2018). The lidar observations (diamonds in Fig. 7) conducted between 11:00–12:00 UTC are in good agreement with the extraordinarily high 500 nm AOT of 1.1 at 10:06 UTC. According to our lidar observations, cirrus clouds were absent during the noon hours of 22 August 2017 so that the shown AERONET smoke observations were not affected by any cloud occurrence.

As can be seen in Fig. 7, the 500 nm FMF increased from values below 0.7 in the early morning of 21 August to values close to 1 when the smoke layers arrived and dominated from noon on 21 August to the evening of 22 August. Accordingly, the total AOT was almost equal to the fine-mode AOT caused by anthropogenic haze in the PBL and the smoke in the free troposphere and stratosphere. The Ångström exponent (for the spectral range from 440–870 nm) was mostly between 1.1–1.4 which is indicative for the presence of a pronounced particle accumulation mode (particles with diameter mostly from 200 to 800 nm, see Haarig et al. (2018) for more details).

The boundary-layer 500 nm AOT was around 0.1–0.15 on 21 and 23 August 2017 (before and after the smoke period) and about 0.15–0.2 on 22 August according to the lidar observations at Leipzig. Thus, the fire smoke layers caused a 532 nm AOT close to 1.0 over Leipzig during the noon hours of 22 August 2017.

During the 11:00–12:00 UTC period AERONET 500 nm AOT values ranged from 0.71–0.82 (mean values of 0.76), whereas the lidar-derived 1-hour average 532 nm AOT was 1.1. A realistic lidar ratio of 70 sr was used in the lidar retrieval of the particle extinction profile. This lidar ratio was measured with Raman lidars at Leipzig after sunset on 22 August 2017, but also with the Raman lidar at Hohenpeissenberg (in the night from 21–22 August) and at Kosetice (in the night from 22–23 August). AERONET obviously underestimated the AOT considerably. In Table 2, we summarize several AERONET/lidar comparisons for the three lidar sites used in this study. In all cases, the AERONET 500 nm AOT was significantly lower than the lidar-derived 532 nm AOT. To identify the reason for the bias in Table 2 we provide information about the AOT contributions of the PBL, the free troposphere (FT), and the lower stratosphere (S). As can be seen, the AERONET AOT values are higher than the overall tropospheric AOT contribution. The underestimation of total AOT is thus probably linked to the occurrence of the unusual stratospheric smoke layer.

Strong forward scattering of sun light towards the sun photometer with  $1.2^\circ$  full angle receiver FOV (Holben et al., 1998) seems to be the reason for the underestimation. If small-angle forward scattering is ignored in the AERONET data analysis, the derived (effective) AOT will be much lower than the true (single-scattering-related) AOT when the main aerosol layer (dominating the AOT) is more than 10 km away from the sun photometer. According to Table 2, AERONET underestimated the AOT by about 30–50%.

In contrast to photometers, lidars usually have a very narrow field of view of the order of  $0.2\text{--}1$  mrad ( $0.01\text{--}0.06^\circ$  full angle) so that forward-scattered laser light does not affect the smoke AOT retrieval. As demonstrated by Wandinger et al. (2010), forward scattering effects only affect spaceborne lidar observations of light extinction in mineral dust layers containing large coarse dust particles, i.e. in cases with strong forward scattering of laser light and a lidar more than 500 km away from the dust layers.

It should be mentioned that small and mesoscale horizontal inhomogeneities in the tropospheric and stratospheric aerosol distributions may have also contributed to the discrepancies between the lidar and sun photometer results in Table 2. Furthermore, a perfect match of lidar and photometer measurement periods was often not possible because of cloud occurrence. In addition, Kostice is 115 km away from the Brno AERONET station so that a direct comparison of Kosetice lidar and Brno photometer observations are not very trustworthy. Finally, the selected smoke lidar ratio of 70 sr may have been too high in some cases of the lidar extinction retrieval. But all these influences should lead to statistical variations in the lidar-photometer AOT difference around zero, rather than to a clear bias as observed.

### 3.6 MODIS AOT observations over Leipzig

Finally, we analyzed MODIS data around Leipzig. The results are shown in Fig. 8. The MODIS 550 nm AOT values confirm the lidar observation. Many 550 nm AOT values were found above 1.0 during the overflight time (close to 8:15 UTC and 12:00 UTC). The cloud fields in Fig. 8a provide an impression of the cumulus cloud distribution in the morning of 22 August 2017 (10:15 local time) which hampered the AERONET observations and the MODIS retrieval efforts. Only a few AOT values for  $3\text{ km}\times 3\text{ km}$  pixels could be retrieved from the MODIS observations. However, these few AOT values in Figs. 8a and 8b clearly point to AOT values of the order of 1.0 (and higher) at 550 nm in the Leipzig area.

## 25 4 Discussion

In Sect. 1, we introduced Table 1 to compare the influence of major and moderate volcanic eruptions and extreme and more common pyrocumulonimbus-related biomass-burning events on the aerosol conditions in the lower stratosphere at northern midlatitudes. The goal was to highlight the tremendous contamination of the lower stratosphere with wildfire smoke over central Europe on 21–22 August 2017.

30 However, there is not doubt that major volcanic eruptions have by far the largest impact on weather and climate. After the Pinatubo eruption, the sulfuric-acid aerosol was distributed over both hemispheres (Sakai et al., 2016) and the 500 nm AOT at northern mid latitudes was  $>0.1$  for more than two years. Particles were present from the tropopause to about 25 km height for

several years. In contrast, even the extremely large stratospheric smoke contributions caused a mean 532 nm AOT (for the 30-60°N region and for the period from 16 August to 3 September 2017) of the order of 0.01-0.015 only (Khaykin et al., 2018). This AOT is comparable with stratospheric AOT values caused by moderate volcanic eruptions (see Table 1). The vertical extent of the detected smoke layers over Europe in August 2017 was typically <2 km and thus small compared to the vertical extent of the thick Pinatubo aerosol layers of more than 10 km in 1991–1993 (Ansmann et al., 1997).

Furthermore, pronounced and dense Pinatubo aerosol layers reached central Europe about 4–6 months after the eruption as a result of the likewise slow meridional air mass transport in the stratosphere from the tropics (<20°N) to lidar sites at >50°N. In contrast, stratospheric particles related to moderate volcanic eruptions and wildfire events at northern midlatitudes are usually advected to central Europe within less than two weeks with the dominating westerly winds (Mattis et al., 2010) so that in these cases almost the maximum impact on the stratospheric aerosol conditions is observable with lidars in Europe. The maximum impact of the Pinatubo aerosol was visible with lidars over Hawaii (DeFoor et al., 1992; Barnes and Hoffmann, 1997) only, about 4–6 weeks after the eruption. The maximum stratospheric Pinatubo-related 550 nm AOT was of the order of 1–1.5 and respective maximum AEC values were of the order of 100–200 Mm<sup>-1</sup> over tropical regions (Shallcross et al., 2018).

Nevertheless, the results in Sect. 3 and Table 1 clearly show to what extent wildfires in combination with thunderstorm activity can pollute the lower stratosphere at mid and high northern latitudes and thus can influence radiative transfer, stratospheric circulation and air flow, cirrus formation, and chemical processes. Since the lifting of smoke within convective cumulus towers is so fast (from the fire sources at ground to the upper troposphere and lower stratosphere within <1 hour) (Rosenfeld et al., 2007), and only a minor part of the huge amount of smoke particles can be activated to nucleated cloud droplets at these extremely polluted conditions (personal communication, Daniel Rosenfeld, April 2018), most of the smoke particles reach the tropopause region without any interaction with trace gases, other aerosol particles, and cloud drops. Our lidar profile measurements of particle linear depolarization ratio suggest that the majority of the stratospheric smoke particles on 22 August 2017 were uncoated, pure soot particles (Haarig et al., 2018).

In Table 1, we included the extraordinarily strong pyrocumulonimbus-related Australian wildfire event observed in February 2009 (Siddaway and Petelina, 2011; de Laat et al., 2012). Strong bushfires, very high temperatures, low winds and thunderstorm evolution on 7 February 2009 (Black Saturday) triggered lifting of enormous amounts of smoke towards the upper troposphere from where the smoke layers ascended by the self-lifting mechanism to 15-20 km height (Boers et al., 2010; de Laat et al., 2012). Similar maximum 532 nm AEC and AOT values as measured over central Europe on 21–22 August 2017 were observed with the CALIPSO lidar in the lower stratosphere over the South Pacific east of Australia at heights above the tropopause and below 20 km a few days after 7 February 2009 (de Laat et al., 2012). The stratospheric perturbation slowly decreased during the following months (February-June 2009) (Siddaway and Petelina, 2011).

Note finally, that most of the AEC and AOT values in Table 1 are based on standard (elastic-backscatter) lidar observations which enable the retrieval of profiles of the particle backscatter coefficient and the particle backscatter ratio only. A direct measurement of the climate-relevant particle extinction coefficient is not possible with standard lidars. A few Raman lidar studies were available (Ansmann et al., 1997; Mattis et al., 2010) providing direct AEC and AOT measurements as well as measured extinction-to-backscatter ratios (lidar ratios). In Table 1, we used lidar ratios of 25 sr (Pinatubo) (Jäger and Dëshler,

2003), 35 sr (moderate volcanic events) (Mattis et al., 2010), and 50 sr during quiet, non-volcanic times (Khaykin et al., 2017) to convert the 532 nm backscatter ratios and backscatter coefficients (derived from the standard backscatter lidar observation) to AEC and AOT values.

## 5 Conclusions

5 Extreme levels of Canadian fire smoke were observed in the stratosphere, 2–5 km above the local tropopause over central Europe on 21–22 August 2017. Extinction coefficients reached values of  $500 \text{ Mm}^{-1}$  and were thus about a factor of 20 higher than maximum extinction values found over Germany after the Pinatubo eruption. These rather high stratospheric extinction coefficients were caused by an extraordinarily strong pyrocumulonimbus event over British Columbia in western Canada on 12 August 2017. Several heavy thunderstorms developed over areas with strong wildfires. We analyzed AERONET, MODIS, 10 OMI, and lidar observations to document this historical, record-breaking stratospheric smoke event in terms of 354 nm aerosol index, and 500–500 nm particle extinction coefficients and optical depths. In an accompanying paper (Haarig et al., 2018), we will deepen the smoke characterization towards microphysical, morphological, and composition-related properties based on observations with three polarization/Raman lidar observations at Leipzig after sunset on 22 August 2017.

This extreme stratospheric aerosol event demonstrates that large amounts of wildfire smoke can reach and pollute the lower 15 stratosphere. Such dense smoke layers sensitively disturb chemical processes, radiative fluxes, and even heterogeneous ice formation in the upper troposphere and this probably over weeks to several months. The black carbon aerosol partly enriches the natural soot particle reservoir between 20–30 km by upward motions (Renard et al., 2008).

The unprecedented stratospheric smoke event (observed with EARLINET lidars throughout Europe from mid August 2017 to January-February 2018) provides a favorable opportunity to validate atmospheric circulation models and to improve smoke 20 transport parameterizations. Modeling of the complex life cycle of soot particles (injection, transport, removal by sedimentation, ascent by self-lifting and gravito-photophoresis effects) and the complex direct and indirect climatic influences is a challenging effort, but of great importance to improve future-climate predictions and to better understand aerosol-cloud interaction in the upper troposphere. However, high quality and trustworthy modeling is only possible in close connection with vertical profiling of aerosol by means of lidar providing smoke injection heights, smoke burden, size distribution, optical 25 properties, and smoke decay and removal behavior, and all this separately for tropospheric and stratospheric heights.

The spread of smoke was monitored with EARLINET over months with ground-based lidars from northern Norway to Crete and from Evora, Portugal, to Haifa, Israel. Never before, such a dense network of ground-based advanced lidars have been operated in Europe. A systematic analysis of all measurements is planned. Spaceborne CALIPSO and CATS (Cloud Aerosol Transport System, <https://cats.gsfc.nasa.gov/data/>) lidar observations will be included in the analysis.

30 A special goal will be the study of the ascent of the soot layers with time. In August 2017, the layers were about 2–4 km above the tropopause, weeks to months later they were mostly observed at heights  $>20$  km, and thus more than 10 km above the tropopause. As mentioned, upward movements of soot containing layers can be the result of heating of the environmental air masses by solar absorption by the soot particles (self-lifting mechanism) and/or by gravito-photophoresis effects.

## 6 Data availability

The Polly lidar data are available at TROPOS upon request (info@tropos.de). Backward trajectories analysis has been supported by air mass transport computation with the NOAA (National Oceanic and Atmospheric Administration) HYSPLIT (Hybrid Single-Particle Lagrangian Integrated Trajectory) model (HYSPLIT, 2018) using GDAS meteorological data (Stein et al., 2015; Rolph et al., 2017). AERONET sun photometer AOT data are downloaded from the AERONET web page (AERONET, 2018). We used the ftp site for MODIS data download: [https://ladsweb.modaps.eosdis.nasa.gov/allData/6/MOD04\\_3K/](https://ladsweb.modaps.eosdis.nasa.gov/allData/6/MOD04_3K/) (MODIS, 2018). OMI AI and MODIS AOT maps (August 2017 mean value) were produced with the GIOVANNI online data system, developed and maintained by the NASA GES DISC (Acker and Leptoukh, 2007). We used active fire products from the MODIS (MCD14DL product) in shapefile formats (<https://earthdata.nasa.gov/earth-observation-data/near-real-time/firms/active-fire-data>).

*Acknowledgements.* The authors gratefully acknowledge the NOAA Air Resources Laboratory (ARL) for the provision of the HYSPLIT transport and dispersion model. We are also grateful to AERONET for providing high quality sun photometer observations, calibrations, and products. Special thanks to the Lindenberg and Brno AERONET teams to carefully run the stations. We also acknowledge the MODIS mission scientists and associated NASA personnel for the production of the data used in this research effort. This activity is supported by ACTRIS Research Infrastructure (EU H2020-R&I) under grant agreement no. 654109. The development of the lidar inversion algorithm was supported by the Russian Science Foundation (project 16-17-10241).

## References

- Acker, J. G., and Leptoukh, G.: Online analysis enhances use of NASA Earth Science Data, *Eos, Trans. AGU*, 88, 2, 14–17, 2007.
- AERONET: AERONET aerosol data base, available at: <http://aeronet.gsfc.nasa.gov/>, last access: 20 February, 2018.
- Althausen, D., Engelmann, R., Baars, H., Heese, B., Ansmann, A., Müller, D., and Komppula, M.: Portable Raman Lidar PollyXT for Automated Profiling of Aerosol Backscatter, Extinction, and Depolarization, *J. Atmos. Oceanic Tech.*, 26, 2366–2378, doi:10.1175/2009JTECHA1304.1, 2009.
- Ansmann, A., Mattis, I., Wandinger, U., Wagner, F., Reichardt, J., and Deshler, T.: Evolution of the Pinatubo Aerosol: Raman Lidar Observations of Particle Optical Depth, Effective Radius, Mass, and Surface Area over Central Europe at 53.48°N, *J. Atmos. Sci.*, 54, 2630–2641, [https://doi.org/10.1175/1520-0469\(1997\)054<2630:EOTPAR>2.0.CO;2](https://doi.org/10.1175/1520-0469(1997)054<2630:EOTPAR>2.0.CO;2), 1997.
- 10 Baars, H., Kanitz, T., Engelmann, R., Althausen, D., Heese, B., Komppula, M., Preißler, J., Tesche, M., Ansmann, A., Wandinger, U., Lim, J.-H., Ahn, J. Y., Stachlewska, I. S., Amiridis, V., Marinou, E., Seifert, P., Hofer, J., Skupin, A., Schneider, F., Bohlmann, S., Foth, A., Bley, S., Pfüller, A., Giannakaki, E., Lihavainen, H., Viisanen, Y., Hooda, R. K., Pereira, S. N., Bortoli, D., Wagner, F., Mattis, I., Janicka, L., Markowicz, K. M., Achtert, P., Artaxo, P., Pauliquevis, T., Souza, R. A. F., Sharma, V. P., van Zyl, P. G., Beukes, J. P., Sun, J., Rohwer, E. G., Deng, R., Mamouri, R.-E., and Zamorano, F.: An overview of the first decade of PollyNET: an emerging network of automated
- 15 Raman-polarization lidars for continuous aerosol profiling, *Atmos. Chem. Phys.*, 16, 5111–5137, doi:10.5194/acp-16-5111-2016, 2016.
- Barnes, J. E., and Hofmann, D. J.: Lidar measurements of stratospheric aerosol over Mauna Loa Observatory, *Geophys. Res. Letts*, 24, 1923–1926, <https://doi.org/10.1029/97GL01943>, 1997.
- Berrick, S., Leptoukh, G., Farley, J., and Rui, H.: Giovanni: A Web services workflow-based data visualization and analysis system, *IEEE Trans. Geosci. Remote Sens.*, 47, 106–113, doi:10.1109/TGRS.2008.2003183, 2009
- 20 Boers, R., de Laat, A. T., Stein Zweers, D. C., and Dirksen, R. J.: Lifting potential of solar-heated aerosol layers, *Geophys. Res. Lett.*, 37, L24802, doi:10.1029/2010GL045171, 2010.
- Buchard, V., da Silva, A. M., Colarco, P. R., Darmenov, A., Randles, C. A., Govindaraju, R., Torres, O., Campbell, J., and Spurr, R.: Using the OMI aerosol index and absorption aerosol optical depth to evaluate the NASA MERRA Aerosol Reanalysis, *Atmos. Chem. Phys.*, 15, 5743–5760, <https://doi.org/10.5194/acp15-5743-2015>, 2015.
- 25 Cheremisin, A. A., Vassilyev, Yu. V., and Horvath, H.: Gravitophoresis and aerosol stratification in the atmosphere, *J. Aerosol. Sci.*, 36, 1277–1299, doi:10.1016/j.jaerosci.2005.02.003, 2005.
- China, S., Scarnato, B., Owen, R. C., Zhang, B., Ampadu, M. T., Kumar, S., Dzepina, K., Dziobak, M. P., Fialho, P., Perlinger, J. A., Hueber, J., Helmig, D., Mazzoleni, L. R., and Mazzoleni, C.: Morphology and mixing state of aged soot particles at a remote marine free troposphere site: Implications for optical properties, *Geophys. Res. Lett.*, 42, 1243–1250, doi: 10.1002/2014GL062404, 2015.
- 30 Dahlkötter, F., Gysel, M., Sauer, D., Minikin, A., Baumann, R., Seifert, P., Ansmann, A., Fromm, M., Voigt, C., and Weinzierl, B.: The Pagami Creek smoke plume after long-range transport to the upper troposphere over Europe – aerosol properties and black carbon mixing state, *Atmos. Chem. Phys.*, 14, 6111–6137, <https://doi.org/10.5194/acp-14-6111-2014>, 2014.
- DeFoor, T. E., Robinson, E., and Ryan, S.: Early lidar observations of the June 1991 Pinatubo eruption plume at Mauna Loa Observatory, *Hawaii Geophys. Res. Letts.*, 19, 187–190, <https://doi.org/10.1029/91GL02791>, 1992
- 35 de Laat, A. T. J., Stein Zweers, D. C., Boers, R., and Tuinder, O. N. E.: A solar escalator: Observational evidence of the self-lifting of smoke and aerosols by absorption of solar radiation in the February 2009 Australian Black Saturday plume, *J. Geophys. Res.*, 117, D04204, doi:10.1029/2011JD017016, 2012.

- Dubovik, O., Sinyuk, A., Lapyonok, T., Holben, B., Mishchenko, M., Yang, P., Eck, T., Volten, H., Muñoz, O., Veihelmann, B., van der Zande, W. J., Leon, J. F., Sorokin, M., and Slutsker, I.: Application of spheroid models to account for aerosol particle non-sphericity in remote sensing of desert dust, *J. Geophys. Res.*, 111, D11208, doi:10.1029/2005JD006619, 2006.
- Engelmann, R., Kanitz, T., Baars, H., Heese, B., Althausen, D., Skupin, A., Wandinger, U., Komppula, M., Stachlewska, I. S., Amiridis, V., Marinou, E., Mattis, I., Linné, H., and Ansmann, A.: The automated multiwavelength Raman polarization and water-vapor lidar PollyXT: the neXT generation, *Atmos. Meas. Tech.*, 9, 1767-1784, doi:10.5194/amt-9-1767-2016, 2016.
- Fernald, F. G.: Analysis of atmospheric lidar observations: some comments, *Appl. Opt.*, 23, 652-653, doi.org/10.1364/AO.23.000652, 1984.
- Freeborn, P. H., Wooster, M. J., Roy, D. P., Cochrane, M. A.: Quantification of MODIS fire radiative power (FRP) measurement uncertainty for use in satellite-based active fire characterization and biomass burning estimation, *Geophys Res. Letts.*, 41, 1988-1994, doi:10.1002/2013GL059086, 2014.
- Fromm, M., Alfred, J., Hoppel, K., Hornstein, J., Bevilacqua, R., Shettle, E., Servranckx, R., Li, Z., Stocks, B.: Observations of boreal forest fire smoke in the stratosphere by POAM III, SAGE II, and lidar in 1998, *Geophys. Res. Lett.*, 27, 1407-1410, 2000.
- Fromm, M. D., and Servranckx, R.: Transport of forest fire smoke above the tropopause by supercell convection, *Geophys. Res. Lett.*, 30, 1542, doi:10.1029/2002GL016820, 2003.
- Fromm, M., Lindsey, D. T., Servranckx, R., Yue, G., Trickl, T., Sica, R., Doucet, P., and Godin-Beekmann, S. E.: The untold story of pyrocumulonimbus, *B. Am. Meteorol. Soc.*, 91, 1193-1209, doi:10.1175/2010bams3004.1, 2010.
- GDAS: Global Data Assimilation System, meteorological data base, available at: <https://www.ready.noaa.gov/gdas1.php>, last access: 20 February, 2018.
- Haarig, M., Ansmann, A., Baars, H., Jimenez, C., Veselovskii, I., Engelmann, R., and Althausen, D.: Triple-wavelength depolarization and lidar-ratio observations at the Leipzig EARLINET site during the record-breaking Canadian wildfire smoke event on 22 August 2017: *Atmos. Chem. Phys. Disc.*, 17, acp-2018-358, 2018.
- Hammer, M. S., Martin, R. V., van Donkelaar, A., Buchard, V., Torres, O., Ridley, D. A., and Spurr, R. J. D.: Interpreting the ultraviolet aerosol index observed with the OMI satellite instrument to understand absorption by organic aerosols: implications for atmospheric oxidation and direct radiative effects, *Atmos. Chem. Phys.*, 16, 2507-2523, <https://doi.org/10.5194/acp16-2507-2016>, 2016.
- Hammer, M. S., Martin, R. V., Li, C., Torres, O., Manning, M., and Boys, B. L.: Insight into global trends in aerosol composition from 2005 to 2015 inferred from the OMI Ultraviolet Aerosol Index, *Atmos. Chem. Phys.*, 18, 8097-8112, <https://doi.org/10.5194/acp-18-8097-2018>, 2018.
- Holben, B. N., Eck, T. F., Slutsker, I., Tanré, D., Buis, J. P., Setzer, A., Vermote, E., Reagan, J. A., Kaufman, Y. J., Nakajima, T., Lavenu, F., Jankowiak, I., and Smirnov, A.: AERONET – a federated instrument network and data archive for aerosol characterization, *Remote Sens. Environ.*, 66, 1-16, 1998.
- Hoose, C. and Möhler, O.: Heterogeneous ice nucleation on atmospheric aerosols: a review of results from laboratory experiments, *Atmos. Chem. Phys.*, 12, 9817-9854, <https://doi.org/10.5194/acp-12-9817-2012>, 2012.
- Hu, Q., Bravo Aranda, J.-A., Popovici, I., Goloub, P., Povdin, T., Veselovskii, I., and Pitras, C.: Observations and analysis of UTLS aerosols detected over North France, *J. Geophys. Res.*, in revision, 2018.
- HYSPLIT: HYbrid Single-Particle Lagrangian Integrated Trajectory model, backward trajectory calculation tool, available at: [http://ready.arl.noaa.gov/HYSPLIT\\_traj.php](http://ready.arl.noaa.gov/HYSPLIT_traj.php), last access: 20 February, 2018.
- Ichoku, C., Giglio, L., Wooster, M. J., and Remer, L. A.: Global characterization of biomass-burning patterns using satellite measurements of fire radiative energy, *Remote Sens. Environ.*, 112, 2950-2962, doi:10.1016/j.rse.2008.02.009, 2008.

- Jäger, H., and Deshler, T.: Correction to Lidar backscatter to extinction, mass and area conversions for stratospheric aerosols based on midlatitude balloonborne size distribution measurements, *Geophys. Res. Lett.*, 30, 7, 1382, doi: 10.1029/2003GL0171892003, 2003.
- Jäger, H.: Long-term record of lidar observations of the stratospheric aerosol layer at Garmisch-Partenkirchen, *J. Geophys. Res.*, 110, D08106, doi:10.1029/2004JD005506, 2005.
- 5 Jensen, E. J., and Toon, O. B.: The potential effects of volcanic aerosols on cirrus cloud microphysics, *Geophys. Res. Lett.*, 19, 1759–1762, <http://dx.doi.org/10.1029/92GL01936>, 1992.
- Khaykin, S. M., Godin-Beekmann, S., Keckhut, P., Hauchecorne, A., Jumelet, J., Vernier, J.-P., Bourassa, A., Degenstein, D. A., Rieger, L. A., Bingen, C., Vanhellemont, F., Robert, C., DeLand, M., and Bhartia, P. K.: Variability and evolution of the midlatitude stratospheric aerosol budget from 22 years of ground-based lidar and satellite observations, *Atmos. Chem. Phys.*, 17, 1829-1845, [https://doi.org/10.5194/acp-](https://doi.org/10.5194/acp-17-1829-2017)  
10 17-1829-2017, 2017.
- Khaykin, S. M., Godin-Beekmann, S., Hauchecorne, A., Pelon, J., Ravetta, F., and Keckhut, P.: Stratospheric smoke with unprecedentedly high backscatter observed by lidars above southern France, *Geophys. Res. Lett.*, 45, <https://doi.org/10.1002/2017GL076763>, 2018.
- Kitzberger, T., Falk, D. A., Swetnam, T. W., and Westerling, L.: Heterogeneous responses of wildfire annual area burned to climate change across western and boreal North America, *PLOS One*, 12, e0188486. doi:<https://doi.org/10.1371/journal.pone.0188486>, 2017.
- 15 Levy, R. C., Remer, L. A., Kleidman, R. G., Mattoo, S., Ichoku, C., Kahn, R., and Eck, T. F.: Global evaluation of the Collection 5 MODIS dark-target aerosol products over land, *Atmos. Chem. Phys.*, 10, 10399-10420, doi:10.5194/acp-10-10399-2010, 2010.
- Levy, R. C., Mattoo, S., Munchak, L. A., Remer, L. A., Sayer, A. M., Patadia, F., and Hsu, N. C.: The Collection 6 MODIS aerosol products over land and ocean, *Atmos. Meas. Tech.*, 6, 2989-3034, doi:10.5194/amt-6-2989-2013, 2013.
- Levy, R., Hsu, C., et al.: MODIS Atmosphere L2 Aerosol Product. NASA MODIS Adaptive Processing System, Goddard Space Flight  
20 Center, USA: [http://dx.doi.org/10.5067/MODIS/MOD04\\_L2.006](http://dx.doi.org/10.5067/MODIS/MOD04_L2.006), 2015.
- Liu, X., and Penner, J. E.: Effect of Mount Pinatubo H<sub>2</sub>SO<sub>4</sub>/H<sub>2</sub>O aerosol on ice nucleation in the upper troposphere using a global chemistry and transport model, *J. Geophys. Res.*, 107(D12), doi:10.1029/2001JD000455, 2002.
- Liu, Y., Stanturf, J.A., and Goodrick, S.L.: Trends in global wildfire potential in a changing climate, *For. Ecol. Manage.*, 259, 685–697, doi:10.1016/j.foreco.2009.09.002, 2009.
- 25 Liu, Y., Goodrick, S., and Heilman, W.: Wildland fire emissions, carbon, and climate: Wildfire-climate interactions, *For. Ecol. Manage.*, 317, 80–96, <http://dx.doi.org/10.1016/j.foreco.2013.02.020>, 2014.
- Mattis, I., Ansmann, A., Wandinger, U., and Müller, D.: Unexpectedly high aerosol load in the free troposphere over Central Europe in spring/summer 2003, *Geophys. Res. Lett.*, 30, 2178, doi:10.1029/2003GL018442, 2003.
- Mattis, I., Müller, D., Ansmann, A., Wandinger, U., Preißler, J., Seifert, P., and Tesche, M.: Ten years of multiwavelength Raman lidar  
30 observations of free-tropospheric aerosol layers over central Europe: Geometrical properties and annual cycle, *J. Geophys. Res.*, 113, D20202, doi:10.1029/2007JD009636, 2008.
- Mattis, I., Seifert, P., Müller, D., Tesche, M., Hiebsch, A., Kanitz, T., Schmidt, J., Finger, F., Wandinger, U., and Ansmann, A.: Volcanic aerosol layers observed with multiwavelength Raman lidar over central Europe in 2008–2009, *J. Geophys. Res.*, 115, D00L04, doi:10.1029/2009JD013472, 2010.
- 35 MODIS: MODIS ftp site for data download: [https://ladsweb.modaps.eosdis.nasa.gov/allData/6/MOD04\\_3K/](https://ladsweb.modaps.eosdis.nasa.gov/allData/6/MOD04_3K/), last access: 19 February, 2018.
- O’Neill, N. T., Eck, T. F., Smirnov, A., Holben, B. N., and Thulasiraman, S.: Spectral discrimination of coarse and fine mode optical depth, *J. Geophys. Res.*, 108, 4559, doi:10.1029/2002JD002975, 2003.

- Pappalardo, G., Amodeo, A., Apituley, A., Comeron, A., Freudenthaler, V., Linné, H., Ansmann, A., Bösenberg, J., D'Amico, G., Mattis, I., Mona, L., Wandinger, U., Amiridis, V., Alados-Arboledas, L., Nicolae, D., and Wiegner, M.: EARLINET: towards an advanced sustainable European aerosol lidar network, *Atmos. Meas. Tech.*, 7, 2389–2409, doi:10.5194/amt-7-2389-2014, 2014.
- Peterson, D. A., Hyer, E. J., Campbell, J. R., Solbrig, J. E., and Fromm, M. D.: A conceptual model for development of intense pyrocumulonimbus in western North America, *Mon. Wea. Rev.*, 145, 2235–2255, doi.org/10.1175/MWR-D-16-0232.1, 2017.
- Pueschel, R. F., Verma, S., Rohatschek, H., Ferry, G. V., Boiadjieva, N., Howard, S. D., and Strawa, A. W.: Vertical transport of anthropogenic soot aerosol into the middle atmosphere, *J. Geophys. Res.*, 105(D3), 3727–3736, doi:10.1029/1999JD900505, 2000.
- Remer, L.A., Mattoo, S., Levy, R. C., and Munchak, L. A.: MODIS 3 km aerosol product: algorithm and global perspective, *Atmos. Meas. Tech.*, 6, 1829-1844. doi:10.5194/amt-6-1829-2013, 2013.
- 10 Renard, J.-B., Ovarlez, J., Berthet, G., Fussen, D., Vanhellemont, F., Brogniez, C., Hadamcik, E., Chartier, M., and Ovarlez, H.: Optical and physical properties of stratospheric aerosols from balloon measurements in the visible and near-infrared domains. III. Presence of aerosols in the middle stratosphere, *Appl. Opt.*, 44, 4086 – 4095, doi:10.1364/ AO.44.004086, 2005.
- Renard, J.-B., Brogniez, C., Berthet, G., Bourgeois, Q., Gaubicher, B., Chartier, M., Balois, J.-Y., Verwaerde, C., Auriol, F., Francois, P., Daugeron, D., and Engrand, C.: Vertical distribution of the different types of aerosols in the stratosphere: Detection of solid particles and analysis of their spatial variability, *J. Geophys. Res.*, 113, D21303, doi:10.1029/2008JD010150, 2008.
- 15 Rohatschek, H.: Levitation of stratospheric and mesospheric aerosols by gravito-photophoresis, *J. Aerosol. Sci.*, 27, 467–475, 1996.
- Rolph, G., Stein, A., and Stunder, B.: Real-time Environmental Applications and Display sYstem: READY. *Environmental Modelling & Software*, 95, 210-228, <https://doi.org/10.1016/j.envsoft.2017.06.025>, 2017.
- Rosenfeld, D., Fromm, M., Trentmann, J., Luderer, G., Andreae, M. O., and Servranckx, R.: The Chisholm firestorm: observed microstructure, precipitation and lightning activity of a pyro-cumulonimbus, *Atmos. Chem. Phys.*, 7, 645-659, <https://doi.org/10.5194/acp-7-645-2007>, 2007.
- 20 Sakai, T., Uchino, O., Nagai, T., Liley, B., Morino, I., and Fujimoto, T.: Long-term variation of stratospheric aerosols observed with lidars over Tsukuba, Japan, from 1982 and Lauder, New Zealand, from 1992 to 2015, *J. Geophys. Res. Atmos.*, 121, 10283-10293, doi: 10.1002/2016JD025132, 2016.
- 25 Sassen, K., Starr, D. O. C. , Mace, G. G., Poellot, M. R., Melfi, S. H., Eberhard, W. L., Spinhirne, J. D., Eloranta, E. W., Hagen, D. E., and Hallett, J.: The 5-6 December 1991 FIRE IFO II jet stream cirrus case study: Possible influences of volcanic aerosols, *J. Atmos. Sci.*, 52, 97-123, 1995.
- Shallcross, S., Mann, G., Neely III, R., Schmidt, A., Marshall, L., Dhomse, S., Haywood, J., Jones, A., Barnes, J., McDermid, S., Carswell, A., and Pal, S.: Global dispersion and microphysical variation of the 1991 Mount Pinatubo plume: A ground-based lidar and interactive modelling analysis, *Atmospheric Chemistry and Physics (ACP)*, in preparation, 2018.
- 30 Siddaway, J. M., and Petelina, S. V.: Transport and evolution of the 2009 Australian Black Saturday bushfire smoke in the lower stratosphere observed by OSIRIS on Odin, *J. Geophys. Res.*, 116, D06203, doi: 10.1029/2010JD015162, 2011.
- Strawa, A. W., Drdla, K., Ferry, G. V., Verma, S., Pueschel, R. F., Yasuda, M., Salawitch, R. J., Gao, R. S., Howard, S. D., Bui, P. T., Loewenstein, M., Elkins, J. W., Perkins, K. K., and Cohen, R.: Carbonaceous aerosol (soot) measured in the lower stratosphere during POLARIS and its role in stratospheric photochemistry, *J. Geophys. Res.*, 104, 26753–26766, doi:10.1029/1999JD900453, 1999.
- 35 Stein, A.F., Draxler, R.R., Rolph, G.D., Stunder, B.J.B., Cohen, M.D., and Ngan, F.: NOAA's HYSPLIT atmospheric transport and dispersion modeling system, *Bull. Amer. Meteor. Soc.*, 96, 2059-2077, <http://dx.doi.org/10.1175/BAMS-D-14-00110.1>, 2015

- Torres, O., Bhartia, P. K., Herman, J. R., and Ahmad, Z.: Derivation of aerosol properties from satellite measurements of backscattered ultraviolet radiation. *Theoretical Basis*, *J. Geophys. Res.*, 103, 17099–17110, doi: 10.1029/98JD00900, 1998.
- Trickl, T., Giehl, H., Jäger, H., and Vogelmann, H.: 35 yr of stratospheric aerosol measurements at Garmisch-Partenkirchen: from Fuego to Eyjafjallajökull, and beyond, *Atmos. Chem. Phys.*, 13, 5205-5225, <https://doi.org/10.5194/acp-13-5205-2013>, 2013.
- 5 Uchino, O., Sakai, T., Nagai, T., Nakamae, K., Morino, I., Arai, K., Okumura, H., Takubo, S., Kawasaki, T., Mano, Y., Matsunaga, T., and Yokota, T.: On recent (2008–2012) stratospheric aerosols observed by lidar over Japan, *Atmos. Chem. Phys.*, 12, 11975-11984, <https://doi.org/10.5194/acp-12-11975-2012>, 2012.
- Wandinger, U., Tesche, M., Seifert, P., Ansmann, A., Müller, D., and Althausen, D.: Size matters: Influence of multiple scattering on CALIPSO light-extinction profiling in desert dust, *Geophys. Res. Lett.*, 37, L10801, doi: 10.1029/2010GL042815, 2010.
- 10 Zhang, Y., Forrister, H., Liu, J., Dibb, J., Anderson, B., Schwarz, J.P., Perring, A. E., Jimenez, J. L., Campuzano-Jost, P., Wang, Y., Nenes, A., and Weber, R. J.: Top-of-atmosphere radiative forcing affected by brown carbon in the upper troposphere, *Nature Geoscience*, 10, 486-489, doi:10.1038/ngeo2960, 2017.
- Zuev, V. V., Burlakov, V. D., Nevzorov, A. V., Pravdin, V. L., Savelieva, E. S., and Gerasimov, V. V.: 30-year lidar observations of the stratospheric aerosol layer state over Tomsk (Western Siberia, Russia), *Atmos. Chem. Phys.*, 17, 3067-3081, [https://doi.org/10.5194/acp-](https://doi.org/10.5194/acp-17-3067-2017)
- 15 17-3067-2017, 2017.

**Table 1.** Comparison of extreme and moderate events of stratospheric aerosol perturbations (volcanic eruptions, pyrocumulonimbus-related smoke events) as observed with lidar over northern midlatitudes. Characteristic values for maximum layer top height (HTOP), typical observable duration of the stratospheric aerosol perturbation (PDUR), maximum 532 nm aerosol extinction coefficient (AEC) and AOT (above the tropopause) are given. For background aerosol conditions, mean AEC and AOT values are shown. The extraordinarily strong (Black Saturday) wildfire smoke event in Australia is included in the comparison. Balloon-borne in situ observations are considered as well (smoke events, background conditions). More explanations are given in Sect. 4.

<b>Perturbation</b>	<b>HTOP</b>	<b>PDUR</b>	<b>AEC</b>	<b>AOT</b>	<b>Reference</b>
<b>Volcanic events</b>					
Major eruption (Mt. Pinatubo, Philippines, June 1991 )	25-35 km	years	25 Mm <sup>-1</sup>	0.2–0.25	Ansmann et al. (1997); Jäger (2005); Trickl et al. (2013); Sakai et al. (2016); Zuev et al. (2017)
Moderate eruption (mid latitudes, tropics)	15-25 km	months	5–15 Mm <sup>-1</sup>	0.02-0.025	Mattis et al. (2010); Uchino et al. (2012); Trickl et al. (2013); Sakai et al. (2016); Khaykin et al. (2017); Zuev et al. (2017)
Quiet periods			0.2–0.6 Mm <sup>-1</sup>	0.004	Jäger (2005); Khaykin et al. (2017)
<b>Smoke events</b>					
Extreme case (Canadian fires, Aug. 2017, Australian fires, Feb. 2009)	15-25 km	months	500 Mm <sup>-1</sup>	0.5-1.0	this study; Khaykin et al. (2018); Siddaway and Petelina (2011); de Laat et al. (2012)
Typical case	15-20 km	days/weeks	20-30 Mm <sup>-1</sup>	0.02	Fromm et al. (2010)
Background conditions			1.5 Mm <sup>-1</sup>	0.005	Renard et al. (2005, 2008)

**Table 2.** Comparison of AOT measured with lidar and AERONET sun photometer on 21-22 August 2017. AERONET level 1.0 (Brno), 1.5 (Hohenpeissenberg, 21 August) and 2.0 (Leipzig, and Hohenpeissenberg, 22 August) are used in the table. AOT contributions of the planetary boundary layer (PBL), the free troposphere (FT), and the stratosphere (S) are separately listed in addition. In the lidar retrieval, a lidar ratio of 60 sr (PBL) and 70 sr (FT, S) is used. Brno is 115 km southeast (1.5 hours downwind at 15 km height on 22 August) of the Kosetice lidar site.

<b>Site and time</b>	<b>PBL</b>	<b>FT</b>	<b>S</b>	<b>AOT(Lidar)</b>	<b>AERONET time</b>	<b>AOT(AERONET)</b>
Hohenpeissenberg (lidar, AERONET)						
21 Aug., 13–13:30 UTC	0.09	0.11	0.42	0.61	13:30-16 UTC	0.32–0.38
22 Aug., 13–15 UTC	0.08	0.03	0.22	0.33	13–15:30 UTC	0.23–0.25
Leipzig (lidar, AERONET)						
22 Aug., 11–12 UTC	0.21	0.30	0.59	1.10	11–12 UTC	0.70–0.84
Kosetice (lidar), Brno (AERONET)						
22 Aug., 15–15:30 UTC	0.24	0.24	0.50	0.98	13:30–17 UTC	0.57–0.73
22 Aug., 18–19 UTC	0.20	0.12	0.47	0.79	17 UTC	0.65
22-23 Aug., 22:30–2 UTC	0.20	0.12	0.28	0.60	5-5:15 UTC	0.45–0.47

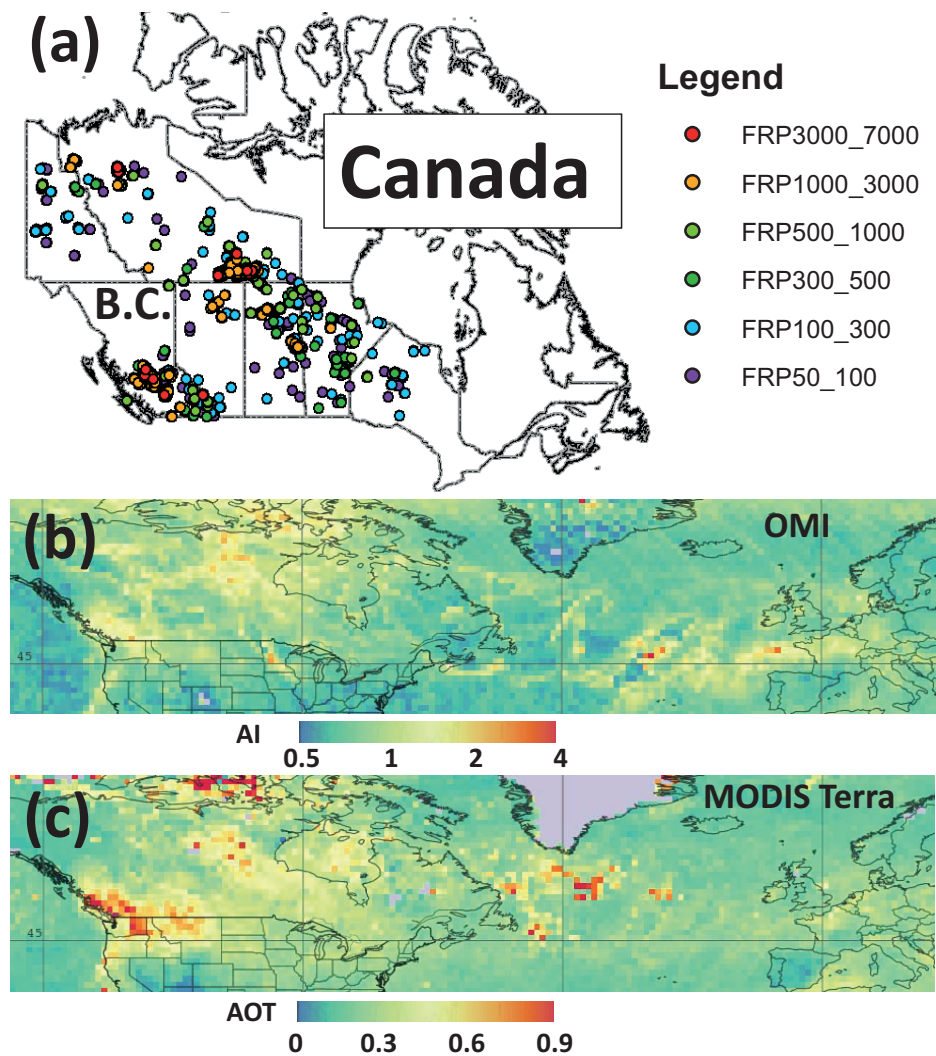


**Figure 1.** (a) Fires detected with MODIS aboard the Terra and Aqua satellites over Canada in the period from 1-31 August 2017. The six color-coded classes of FRP (in MW) indicate different fire strengths (intensity of biomass burning). Intense wildfires accumulated in the southern part of British Columbia (B. C.). (b) August 2017 mean AI (aerosol index, OMI) at 354 nm, and (c) August 2017 mean 550 nm AOT (MODIS) (Acker and Leptoukh, 2007).

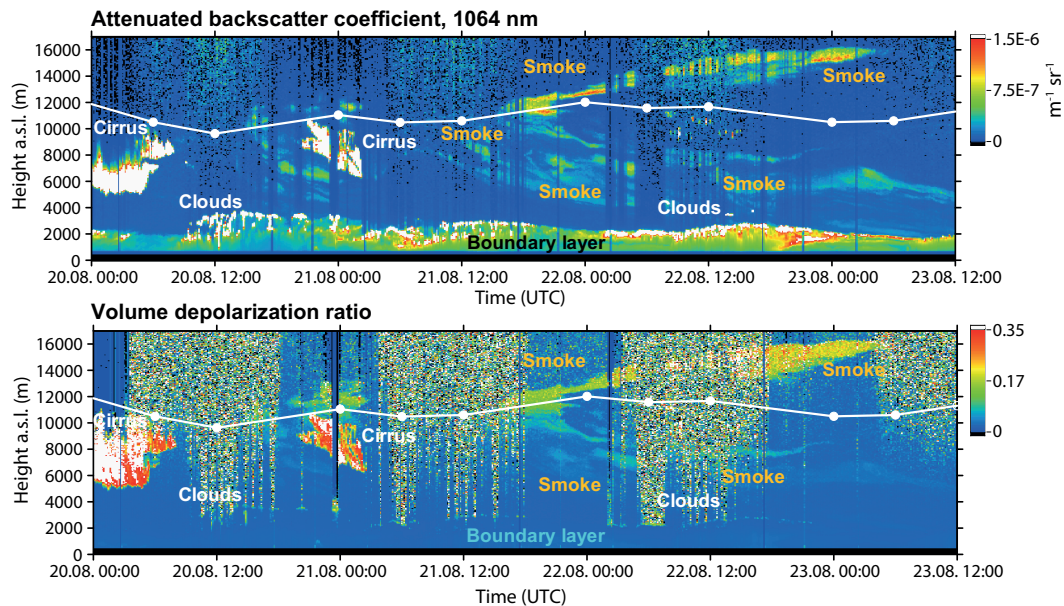


**Figure 2.** Canadian wildfire smoke layers in the troposphere and stratosphere over Kosetice, Czech Republic, observed with lidar on 20–23 August 2017. The uncalibrated attenuated backscatter coefficient (range-corrected signal) at 1064 nm (top) and the volume linear depolarization ratio at 532 nm (bottom) are shown as a function of height above sea level (a.s.l.). Particle extinction coefficients at 532 nm ranged from 250–500  $\text{Mm}^{-1}$  in the stratospheric layer from 12 to 16 km height (21 August, 21:00 UTC to 23 August, 5:00 UTC). The tropopause height according to the Prague radiosonde, launched daily at 00:00, 06:00, and 12:00 UTC (see full circles), is given by white lines.

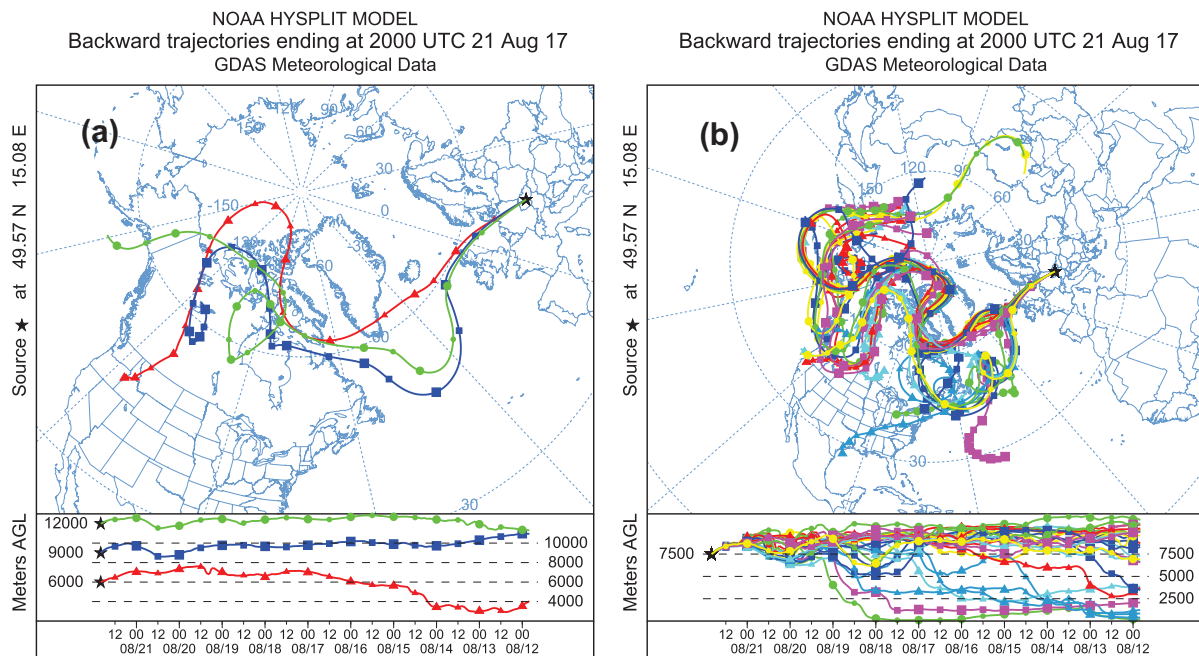


**Figure 3.** 10-day backward trajectories (Stein et al., 2015; HYSPLIT, 2018) arriving at Kosetice, Czech Republic, on 21 August 2017, 20 UTC at (a) 6 km (red), 9 km (blue) and 12 km height (green) above ground level, and (b) ensemble of trajectories for the arrival height of 7.5 km. The trajectories show that the smoke source region is the North American continent.

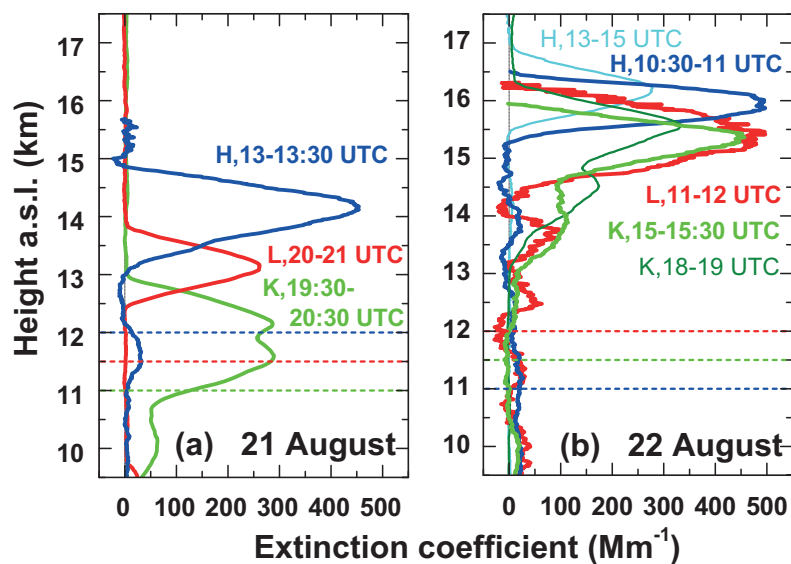


**Figure 4.** Height profile of particle extinction coefficient at 532 nm over Hohenpeissenberg (H), Leipzig (L), and Kosetice (K) on (a) 21 and (b) 22 August 2017. Time periods (in UTC) indicate signal averaging time periods. The Fernald method was applied to compute the extinction profiles. An input lidar ratio of 70 sr (in agreement with nighttime Raman lidar observations of the smoke lidar ratio) was used. The uncertainty in the stratospheric extinction coefficients is estimated to be 15%. The horizontal dashed lines indicate the tropopause heights over the different lidar sites of Hohenpeissenberg (blue), Leipzig (red), and Kosetice (green) estimated from nearby radiosonde temperature and humidity profiles.

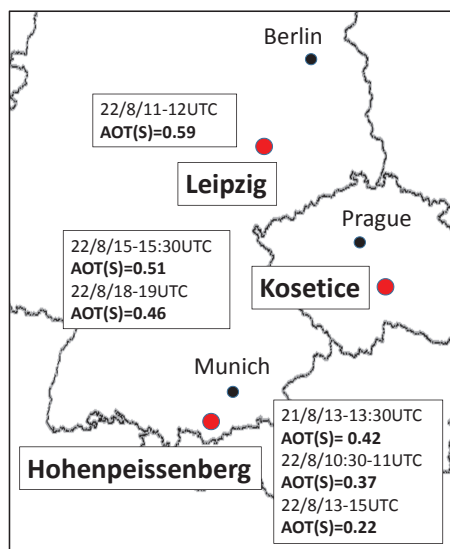


**Figure 5.** Lidar stations (red circles) in Germany and Czech Republic. AOT(S) denotes the AOT at 532 nm of the stratospheric smoke layer as observed on 21 August (21/8) and 22 August 2017 (22/8) for the indicated time periods in UTC.

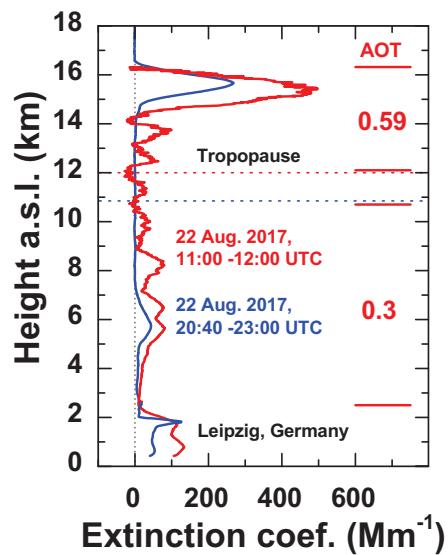


**Figure 6.** Height profile of particle extinction coefficient at 532 nm over Leipzig on 22 August 2017 measured with lidar close to noon (red profile), when the optically densest stratospheric smoke layers crossed the lidar site, and at nighttime (blue profile). The nighttime observations with three lidars will be discussed in detail in Haarig et al. (2018). The data analysis is the same as in Fig 4. The 532 nm AOTs for the free troposphere and lower stratosphere are given as numbers. Horizontal dashed lines indicate the tropopause height around noon and around midnight on 22 August. The uncertainty in the extinction coefficients and AOT values is about 15%.

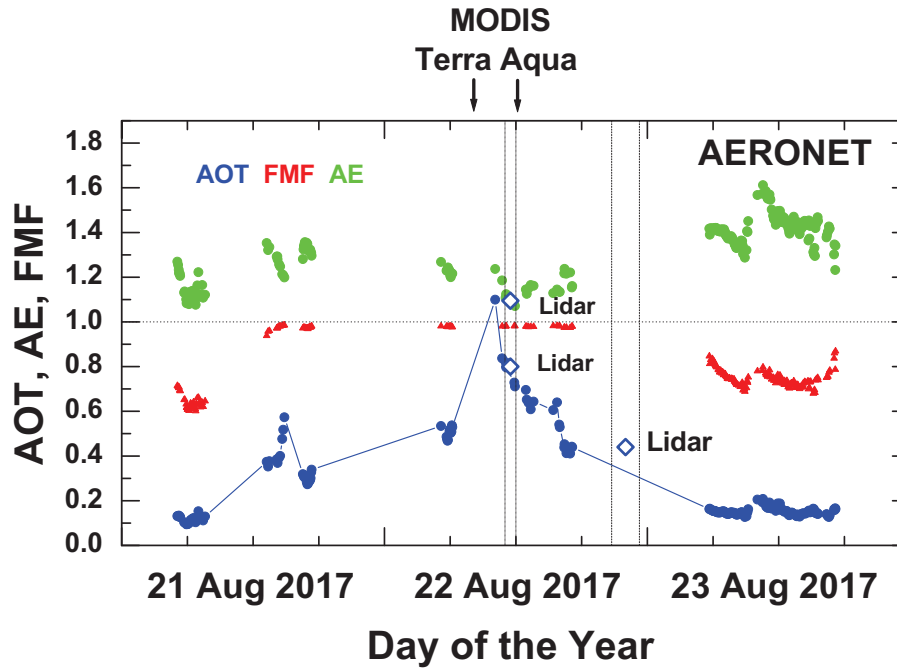


**Figure 7.** AERONET sun photometer observations at Leipzig (TROPOS) from 21–23 August 2017 (level 2.0 data). 500 nm AOT (blue circles), Ångström exponents AE (green circles, for the 440-870 nm wavelength range), and AOT fine-mode fraction FMF (red triangles, for 500 nm AOT) are shown. Gaps in the time series are caused by cloud fields and night time hours. Dashed vertical lines indicate the lidar measurement periods around noon and at nighttime (Fig. 6). The lidar-derived 532 nm AOT (blue open diamonds) are given in addition. AOTs are obtained with an input lidar ratio of 50 sr (AOT of 0.8 on 22 August around noon) and 70 sr (AOT of 1.1 around noon and 0.42 in the night of 22 August). The horizontal line at 1.0 indicates that the FFM values were close to 1.0 during the passage of the smoke layers so that the AOT was almost entirely caused by light extinction by fine mode particles. The overpass times of MODIS Terra and Aqua are indicated above the figure. MODIS results are shown in Fig. 8.

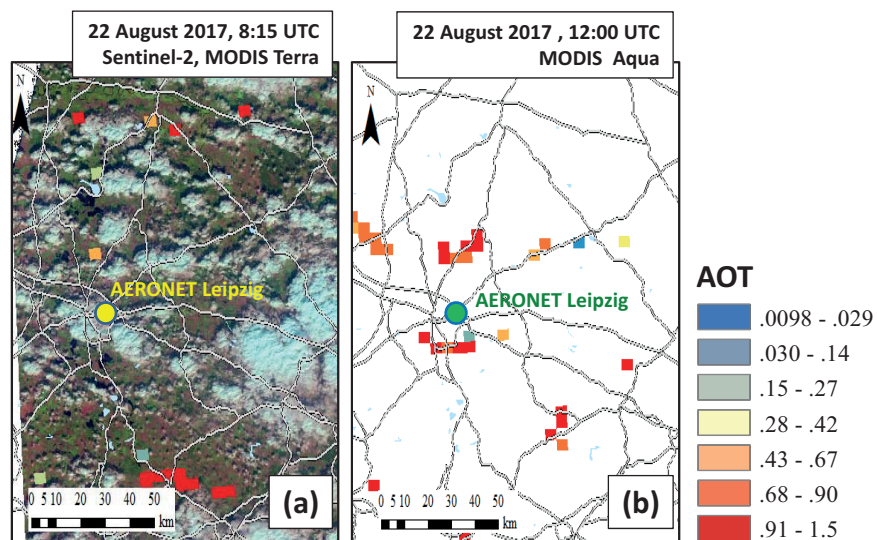


**Figure 8.** (a) Sentinel-2 cumulus cloud fields (bluish-white) for 8:30 UTC equatorial crossing time (Leipzig, overpass at 8:15 UTC), and integrated MODIS Terra color-scaled 550 nm AOT values for 3 km×3 km cloud-free areas, (b) respective MODIS Aqua 550 nm AOT retrievals for 11:30 UTC equatorial crossing time (Leipzig, overpass at 12:00 UTC). The yellow (a) and green (b) circles indicate the AERONET Leipzig site. Many red squares (AOT of 0.9-1.5) were retrieved from the MODIS observations south and north of the AERONET station.